**Universidade de Évora - Escola de Ciências e Tecnologias**

Mestrado Integrado em Medicina Veterinária

Dissertação

# Histological and Immunohistochemical Characterization of the Mammary Gland of Jennets from the Miranda Breed

Rafaela Gomes de Jesus

Orientador(es) | Rita Payan Carreira
Adelina Maria Gaspar Gama Quaresma
Sandra Maria Branco

Évora 2024

**Universidade de Évora - Escola de Ciências e Tecnologias**

Mestrado Integrado em Medicina Veterinária

Dissertação

# Histological and Immunohistochemical Characterization of the Mammary Gland of Jennets from the Miranda Breed

Rafaela Gomes de Jesus

Orientador(es) | Rita Payan Carreira
Adelina Maria Gaspar Gama Quaresma
Sandra Maria Branco

Évora 2024

A dissertação foi objeto de apreciação e discussão pública pelo seguinte júri nomeado pelo Diretor da Escola de Ciências e Tecnologia:

| | | |
|---|---|---|
| Presidente | \| | Maria Eduarda Potes (Universidade de Évora) |
| Vogais | \| | Irina Ferraz Amorim Cruz (Universidade do Porto – Instituto de Ciências Biomédicas Abel Salazar (Arguente) |
| | | Rita Payan-Carreira (Universidade de Évora) (Orientador) |

Évora 2024

**Acknowledgments**

Words cannot express my gratitude to my professors, Dr. Rita Payan Carreira and Dr. Sandra Maria Branco from the University of Évora (UE), and Drs. Adelina Maria Gaspar Gama Quaresma and Miguel Nuno Pinheiro Quaresma from the University of Trás-os-Montes and Alto Douro (UTAD), for their invaluable patience and feedback. I could not have undertaken this journey without them, who generously provided knowledge and expertise. I also reinforce my thanks to Professor Dr. Miguel Nuno Pinheiro Quaresma, who, from 2009 to 2018, collected samples of *"Burro de Miranda"* Breed (BMB) jennets, setting the basis for this study.

Additionally, this endeavour would not have been possible without the generous support from the entire team of professionals and Ph.D. students at the Laboratory of Histology and Pathological Anatomy of the University of Trás-os-Montes and Alto Douro (LHAP-UTAD), who have given me valued assistance during the internship.

I would also like to express gratitude to the veterinarian Rute Vieira, who put the optical microscope of her veterinary clinic at my disposal, which was often used to reanalyze the data collected during the internship at LHAP-UTAD.

Lastly, I would be remiss in not mentioning my family, especially my parents, brother, and boyfriend. Their belief in me has kept my spirits and motivation high during this process. I would also like to thank my dog and cat for all the entertainment and emotional support.

**Abstract**

A comprehensive characterization of the donkey mammary gland (MG) histology supports the investigation of pathological processes affecting this organ. Accordingly, the present study aimed to evaluate asinine MG histomorphology.

Sixty-five MGs collected from jennies (0 to 444 months) were processed for light microscopy. Immunohistochemistry was performed on sixteen samples using AE1AE3, α-smooth muscle actin, p63, calponin and vimentin antibodies. The MGs presented two paired mammary complexes with distinct histological morphologies according to the stage: prepubertal (inactive/quiescent), fully developed lactating, and involuting MG. Ten adult jennies (15.4%) presented: papillomatosis with duct ectasia (3.1%); cystic apocrine metaplasia (1.5%) and sebaceous (9.2%) and apocrine (4.6%) metaplasia, with multiple alterations in two animals. Mineralized concretions (46.1%), mononuclear inflammatory (28,6%) and eosinophils (7,4%) infiltrates were also observed.

Given the immunohistochemical similarities with other mammals, comparative studies on the MG biopathology focusing on donkeys may provide new insights on tumourigenesis, with potential application to other species.

**Keywords**: Donkey; mammary gland; histology; pathology; immunohistochemistry

**Caracterização histológica e imunohistoquímica da glândula mamária de burras da raça de Miranda**


## Resumo

A investigação de processos patológicos que envolvem a glândula mamária (GM), apenas é possível após conhecimento detalhado da sua histomorfologia. Como tal, o presente estudo avaliou a histomorfologia da GM asinina.

Foram processadas para microscopia de luz sessenta e cinco GMs de burras (idades entre 0 e 444 meses), e destas, dezasseis foram submetidas a imunohistoquímica usando AE1AE3, α- actina de músculo liso, p63, calponina e vimentina. As GMs apresentaram dois complexos mamários por teto com características variáveis consoante a fase: pré-púbere (inativa/quiescente), em lactação ou em involução. Dez glândulas mamárias (15.4%) exibiram alterações metaplásicas/proliferativas: papilomatose (3,1%); metaplasia apócrina cística (1,5%) e metaplasia sebácea (9,2%) e apócrina (4,6%), com múltiplas alterações em dois animais. Foram frequentemente observadas concreções mineralizadas (46,1%) e infiltrados inflamatórios mononucleares (28,6%) e eosinofílicos (7,4%).

Consideramos que estudos comparativos sobre a biopatologia da GM asinina possam fornecer novas informações sobre a tumorigénese, com potencial aplicação noutras espécies.



**Palavras-chave:** Asinino; glândula mamária; histologia; patologia; imunohistoquímica

**Index**

Acknowledgments ..... iv
Abstract ..... v
Figures Index ..... ix
Tables Index ..... xi
Appendix Index ..... xi
Abbreviations and Acronyms ..... xii
I – Introduction ..... 1
1. *"Burro de Miranda"* breed (BMB) ..... 1
2. Comparative anatomy and histology ..... 2
2.1 Mammary gland anatomy ..... 3
2.2 Mammary gland histology ..... 4
3. Mammary gland development ..... 9
4. Reproductive cycle and mammary gland histological changes ..... 11
5. Immunohistochemistry and immunohistochemical markers ..... 12
II. Aims ..... 16
III - Materials and Methods ..... 17
1. Samples ..... 17
2. Methods ..... 18
2.1 Histology ..... 18
2.2 Immunohistochemistry ..... 18
2.2.1 Immunohistochemical evaluation ..... 20
3. Analysis ..... 21
IV - Results ..... 22
1. Macroscopic evaluation of jennet's mammary gland ..... 22
2. Histological evaluation of jennet's mammary gland ..... 22
2.1 Mammary gland normal structure ..... 22
2.2 Development of postnatal morphological changes in donkey mammary gland ..... 26
3. Immunohistochemical characterization of the donkey mammary gland ..... 29
3.1 Teat ..... 29
3.2 Mammary parenchyma ..... 32
3.3 Stroma ..... 35
4. Histopathological alterations of donkey mammary gland ..... 37
4.1 Metaplastic/proliferative mammary lesions ..... 37
4.2 Psammoma bodies (PBs) ..... 38

4.3 Mammary gland inflammatory infiltrate ..... 39
4.4 Other alterations ..... 40
V - Discussion ..... 42
1. Macroscopic and microscopic features of jennet mammary gland ..... 42
2. Immunohistochemical characterization of jennet mammary gland ..... 43
2.1 Teat ..... 44
2.2 Mammary parenchyma ..... 46
2.3 Stroma ..... 47
3. Histopathological alterations of donkey mammary gland ..... 49
VI - Conclusion ..... 53
VII - References ..... 55
VIII – Appendix ..... 71

## Figures Index

Figure 1 - Schematic representation of a half udder of a donkey ..... 4
Figure 2 - Schematic diagram of a mammary duct in cross-section ..... 6
Figure 3 - Schematic representation of Equus caballus MG ..... 10
Figure 4 - Schematic representation of a terminal end bud (TEB) ..... 11
Figure 5 - External appearance of BMB jennet's udder and teats.. ..... 21
Figure 6 - External appearance of BMB jennet's udder and teats. ..... 21
Figure 7 - Donkey teat orifices. H&E stain ..... 22
Figure 8 - Donkey teat skin. H&E stain. ..... 22
Figure 9 - Donkey teat canals. H&E stain. ..... 23
Figure 10 - Donkey teat canal and gland cistern. H&E stain. ..... 23
Figure 11 - Donkey lactating MG. H&E stain. ..... 25
Figure 12 – Donkey MG: bilayered epithelium og mammary ducts. H&E stain ..... 25
Figure 13 – Donkey MG: IAS and IES.H&E stain ..... 25
Figure 14 - Newborn donkey MG. H&E stain ..... 26
Figure 15 - Newborn donkey MG: TEBs. H&E stain ..... 26
Figure 16 - Donkey lactating MG. H&E stain. ..... 27
Figura 17 - Donkey lactating MG. H&E stain ..... 27
Figure 18 - Donkey non-lactating MG. H&E stain ..... 28
Figure 19 - Donkey non-lactating MG. H&E stain ..... 28
Figure 20 - Donkey MG with transitional morphology. H&E stain ..... 28
Figure 21 - Donkey MG with transitional morphology. H&E stain ..... 28
Figure 22 - Donkey teat. p63 immunostaining ..... 29
Figure 23 - Donkey teat CK AE1AE3 immunostaining. ..... 29
Figure 24 - Donkey teat Calponin immunostaining ..... 30
Figure 25 - Donkey teat. α-SMA immunostaining ..... 30
Figure 26 - Donkey teat orifices and teat canals. CK AE1AE3 immunostaining ..... 30
Figure 27 - Donkey gland cistern. CK AE1AE3 immunostaining. ..... 30
Figure 28 - Donkey gland cistern. p63 immunostaining ..... 31
Figure 29 - Donkey mammary parenchyma. p63 immunostaining ..... 31
Figure 30 - Donkey gland cistern. α-SMA immunostaining ..... 31
Figure 31 - Donkey mammary parenchyma. Calponin immunostaining ..... 31
Figure 32 – Donkey teat SMS. Vimentin immunostaining ..... 32
Figure 33 – Donkey teat SMS. Calponin immunostaining ..... 32
Figure 34 - Newborn donkey MG: TEBs. CK AE1AE3 Immunostaining. ..... 32
Figure 35 - Newborn donkey MG: TEBs. P63 immunostaining ..... 32

Figure 36 - Newborn donkey MG: TEBs. α-SMA immunostaining ..... 33
Figure 37 - Newborn donkey MG: TEBs. Vimentin immunostaining ..... 33
Figure 38 - Donkey lactating MG. CK AE1AE3 immunostaining. ..... 33
Figure 39 - Donkey lactating MG. CK AE1AE3 immunostaining ..... 33
Figure 40 - Donkey non-lactating MG. CK AE1AE3 Immunostaining ..... 34
Figure 41 - Donkey non-lactating MG. CK AE1AE3 Immunostaining ..... 34
Figure 42 - Donkey lactating MG. α-SMA immunostaining. ..... 34
Figure 43 - Donkey non-lactating MG. α-SMA immunostaining ..... 34
Figure 44 - Donkey Lactating MG. p63 immunostaining ..... 35
Figure 45 - Donkey non-lactating MG. p63 immunostaining ..... 35
Figure 46 - Donkey MG with lobular hyperplasia. Vimentin Immunostaining ..... 35
Figure 47 - Donkey non-lactating MG. Vimentin Immunostaining ..... 35
Figure 48 - Donkey MG: vessels. Vimentin immunostaining ..... 36
Figure 49 - Donkey MG: vessels Calponin immunostaining. ..... 36
Figure 50 - Donkey MG: vessels α-SMA immunostaining ..... 36
Figure 51 - Donkey MG: vessels. α-SMA immunostaining ..... 36
Figure 52 - Donkey MG: Multiple intraductal epithelial papillary projections, associated with duct ectasia.H&E stain ..... 38
Figure 53 - Donkey MG: Cystic apocrine metaplasia, characterized by cystically dilated ducts lined by benign apocrine epithelium. H&E stain ..... 38
Figure 54 - Donkey MG: mammary apocrine and squamous metaplasia. CK AE1AE3 immunostaining ..... 38
Figure 55 - Donkey MG: mammary sebaceous metaplasia. H&E stain ..... 38
Figure 56 - Donkey MG: PBs. H&E stain ..... 39
Figure 57 - Donkey MG:PBs. CK AE1AE3 Immunostaining ..... 39
Figure 58 - Donkey MG: mononuclear inflammatory infiltrate. H&E stain ..... 39
Figure 59 - Donkey MG: mononuclear inflamatory infiltrate. Vimentin Immunostaining 39
Figure 60 -Donkey MG: mononuclear inflamatory infiltrate. H&E stain ..... 40
Figure 61 – Donkey teat skin: eosinophils. H&E stain. ..... 40
Figure 62 - Donkey non-lactating MG: MEC hipertrophy. H&E stain ..... 40
Figure 63 - Donkey non-lactating MG: MEC hipertrophy. H&E stain. ..... 40
Figure 64 - Donkey MG: MEC hiperplasia and hypertrophy. p63 immunostaining. ..... 41
Figure 65 - Donkey MG: MEC hiperplasia and hypertrophy. CK AE1AE3 immunostaining ..... 41

## Tables Index

Table 1 - Different LEC appearances in gland cistern/lactiferous sinus, duct/ductules and alveoli, documented in humans, mice, dogs, and cows. ..... 7
Table 2 - Animal's age and year of collection of the sixteen samples chosen for the indirect immunohistochemistry technique. ..... 17
Table 3 - Antibodies used for immunohistochemical examination of JMG. ..... 20
Table 4 - Positive Control for each immunohistochemical marker. ..... 21
Table 5 - Differential expression of the immunohistochemical markers in teat skin structures. ..... 29
Table 6 - Comprehensive and detailed summary of the main conclusions drawn from analysing different histological appearances of jennet's mammary gland ..... 37

## Appendix Index

Appendix 1 – Scientific poster: Congress of the ECVP/ESVP/ECVCP/ESVCP – Lisbon 2023 ..... 71

## Abbreviations and Acronyms

**AEPGA** - Association for the Study and Protection of Asinine Livestock/ *Associação para o Estudo e Proteção do Gado Asinino*

**APM** – Arrector Pili Muscle

**BMB** – *"Burro de Miranda"* Breed

**CALP** -Calponin

**EMT** – Epithelial-Mesenchymal Transition

**FAO** - Food and Agriculture Organization of the United Nations

**H&E** - Haematoxylin and Eosin

**IAS** – Intralobular Stroma

**IES** – Interlobular Stroma

**IF** - Intermediate Filament

**JMG** – Jennet's Mammary Gland

**LEC** – Luminal Epithelial Cells

**LHAP** – Laboratory of Histology and Veterinary Anatomical Pathology/ Laboratório de Histologia e Anatomia Patológica

**MEC** – Myoepithelial Cells

**MPSU** – Mammo-Pilo-Sebaceous Unit

**PBs** - Psammoma Bodies

**SMC** - Smooth Muscle Cells

**SMF** - Smooth Muscle Fibres

**SMS –** Smooth Muscle Sphincter

**TDLU** - Terminal Ductal Lobular Unit

**TEBS** - Terminal End Buds

**UTAD** – *Trás-os-Montes e Alto Douro* University/ Universidade de Trás-os-Montes e Alto Douro

**VIM** -Vimentin

**α-SMA** - Alpha Smooth Muscle Actin

# I – Introduction

Very little is known about the anatomy and histology of the donkey's (*Equus Asinus*) mammary gland. Raising interest in recent years has been focusing on the use of donkeys' milk for human consumption as a hypoallergenic substitute for children affected by cows' milk protein allergies or multiple food intolerances (Valle et al., 2018; Souroullas et al., 2018; Zhang et al., 2018) and as a potential complementary dairy product for aged people to treat a variety of human diseases, including cancer, due its effects up-regulating the immune system (Salimei & Fantuz, 2012; Li et al., 2020). Therefore, several scientific papers on the composition and microbiological quality of donkey´s milk (Sarno et al., 2012; Colavita et al., 2016; Valle et al., 2018; Li et al., 2019; Martini et al., 2020; Turini et al., 2020), its potential toxicities (Fantuz et al., 2015), optimized milking systems (D'Alessandro et al., 2015; Valle et al., 2018; De Palo et al., 2022) and improvement of the hygienic collection conditions (Pilla et al., 2010), were published. The little information collected about donkey's mammary gland anatomy occurred during studies on the improvement of milking systems, in which measurements of the mammary gland were carried out by direct observation and ultrasonographic methods (D'Alessandro et al., 2015; Hassan et al., 2016; Kaskous & Pfaffl 2022). It is still an area that deserves to be investigated to facilitate the detection of mammary pathologies and apply preventive measures promptly. Accordingly, this study aimed to evaluate the histological and morphological characteristics of donkey's mammary gland, by routine light microscopy and by indirect immunohistochemical technique, with the application of specific tissue markers.

## 1. *"Burro de Miranda"* breed (BMB)

The *"Burro de Miranda"* breed (BMB) is one of the two officially recognized donkey breeds in Portugal. It is an autochthonous breed originated from *Planalto Mirandês* region, located in North-Eastern Portugal (Quaresma, 2005; Quaresma et al., 2014; SPREGA, 2022; Bessa et al. 2021). The breed population markedly decreased by the end of the 70s and throughout the 80s and 90s because of changes in farming practices towards mechanization, the main reason why the

breed is now vulnerable to extinction (Colli *et al*. 2012; Quaresma M. et al., 2014). The breed presents today around 756 females and 60 males registered in the Studbook and falls into the Food and Agriculture Organization of the United Nations (FAO) category of a species in danger of extinction. Although the breed is under a conservation plan and the number of animals has slightly increased in the last decade, the current reproductive rates remain lower enough to reverse the endangered situation, and the animal population is aging. The animals are distributed by around 460 owners (Bessa et al., 2021; SPREGA, 2022; Quaresma et al., 2014).

The Association for the Study and Protection of Asinine Livestock (AEPGA, "*Associação para o Estudo e Proteção do Gado Asinino*"), the national entity responsible for the breed Studbook, was created as part of a global conservation effort. It has been registering animals presenting the breed characteristics and promoting donkey use and welfare since its creation in 2002 and awakens the public interest with events like a traditional donkey market and festivals (Kugle et al., 2008; Quaresma et al., 2014).

## 2. Comparative anatomy and histology

The horse is the phylogenetically closest species to the donkey; therefore, for comparative purposes, we expect similarities between mammary gland anatomy and histology of both species. Unfortunately, there are few published studies on horse mammary histology. The study that served as a comparative basis for ours was that of Hughes (2020a), that described the histology of the teat and udder of the mare's normal mammary gland.

The study of diagnostic methods for neoplastic conditions is more advanced in horses than in donkeys. However, the presence of mammary tumors continues to be quite difficult to diagnose promptly (Shank, 2009; Boyce & Goodwin, 2017; Hughes, 2020b). Clinical signs are often confused with mastitis, and a specific framework for histopathological phenotyping of equine mammary tumours is not well established (Hughes, 2020b).

## 2.1 Mammary gland anatomy

The jennets' udder comprises one pair of inguinal mammae, each usually drained by two independent mammary ductal trees (three may rarely occur), which arise during foetal development, similarly to the mare (Chavatte-Palmer, 2002; Canisso et al., 2020; Hughes, 2020a; Hughes, 2020b). Thus, each teat typically has two orifices through which the primary ducts discharge (Oftedal & Dhouailly, 2013). Likewise, equids, small ruminants such as sheep (*Ovis aries*) and goats (*Capra hircus*) have only one pair of inguinal mammae in contrast with cows that have two. Nonetheless, both have only one ductal system per mammae (Nickerson & Akers, 2011; Koyama et al., 2013; Hughes, 2020a).

The udder shape of the female donkey was classified as 89% "bowl" and 11% "globular", and the teat shape as 78% "conical" and 22% "cylindrical" (Kaskous and Pfaffl, 2022). Each tree-like ductal system is composed of lobules arranged into distinct lobes. Each lobe has its excretory duct, draining milk into the gland cistern, subsequently the teat canal, and finally exiting the teat orifice (D'Alessandro et al., 2015; Kaskous and Pfaffl, 2022). Donkey's gland cistern is characterized by multiple pockets that open directly into the teat duct/cistern (Fig. 1) instead of a single cistern cavity as in cows (Khan et al., 2020). It is known that the equid udder has a lower storage capacity compared with ruminants and is more adapted to frequent milk removal (D'Alessandro et al., 2015; Kaskous and Pfaffl, 2022). In mares, humans (Hughes, 2020a), dogs (Sorenmo et al., 2011; Zappulli et al. 2019), and ruminants (Rowson, 2012) the authors described the alveolar lobules (the secretory portion of the gland) as a terminal ductal lobular unit (TDLU). In mice, the TDLUs are called alveolar buds (AB) (Líška et al., 2016; Cardiff et al.,2018; Barbosa et al., 2018).

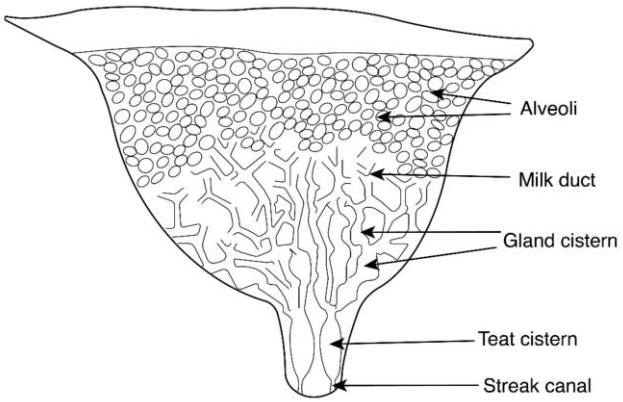


*Figure 1 - Schematic representation of a half udder of a donkey (Kaskous and Pfaffl, 2022).*

## 2.2 Mammary gland histology

### 2.2.1Teat

Little is known about the external appearance of donkey's teat and MG. In horses, Ludewig (1997) emphasized a dark pigmented skin in *corpus mammae*, *sulcus intermammarius* and teat. A dark coloration was observed in dogs and is justified by the presence of melanocytes in the *Stratum Basale*, often with vacuolated cytoplasm (Sorenmo, 2010), which creates a pigmentation on the teat epidermis (Evans & Christensen, 2013). Similarly, teats can also be pigmented in cows, often manifesting as patches of dark and unpigmented epidermis like the broken colour patterns of most dairy breeds' coats (Koyama et al., 2013). In humans, melanocytes are not restricted to the epidermis but are also very abundant in the basal layer of sebaceous glands and lactiferous ducts (Giacometti & Montagna, 1962; Montagna, 1970; Koyama et al., 2013). In mice, Abdalkhani et al. (2002) observed a few melanocytes containing pigment granules in the connective tissue between the teat duct and the epidermis (Koyama et al., 2013). The extension of the teat epidermis showed minimal hair follicles and large adnexal glands in all the mammary areas of dogs (Zappulli et al., 2019), cows (Nickerson & Akers, 2011) and dromedaries (Kausar et al., 2001; Cardiff et al., 2018).

Generally, the common integument (*integumentum commune*) comprises skin, hair, claws, pads, and skin glands, including the skin of MG. Microscopically, the skin (*cutis*) consists of a superficial epidermis of stratified squamous epithelium and the underlying connective tissue, the dermis. The

interface between the epidermis and the dermis is formed by a functional basement membrane of matrix proteins. The skin is underlain by a subcutis (*tela subcutanea* or hypodermis), which is not part of the skin. The subcutis connects the dermis with the fascia and the various forms of hair (pili) that compose the coat (Evans & Christensen, 2013). The epithelium of the nipple/teat is continuous with a keratinized stratified squamous epithelium of the epidermis, resembling the adjacent epidermis in dromedaries (Kausar et al., 2001), horses (Hughes, 2020a), mice (Masso-Welch et al., 2000), humans (Cardiff R. et al.,2018) and dogs (Zappulli et al. 2019).

Regarding epidermis thickness, in horses, Ludewig (1997) mentioned a thicker *stratum corneum* (up to 70 layers of cornified layers) and *stratum spinosum* of the *sulcus intermammarius*. Evans & Christensen (2013) and Zappulli et al. (2019) also commented on differences in the thickness of the epithelium in dogs. While Evans & Christensen (2013) referenced a thin skin layer over the distal teat tip and an increased thickness near the teat base; Zappulli et al. (2019) stated a slightly thicker teat external portion compared to the epidermis of the adjacent skin. The key distinguishing feature of the epidermis between the nipple/teat and the surrounding breast or abdominal skin, of humans (Giacometti & Montagna, 1962; Montagna, 1970; Foley et al., 2001; Doucet et al., 2012; Koyama et al., 2013), cows (Helmboldt et al. 1953), and mice (Mahler et al., 2004), is the epidermal ridges (also named “invaginated folds” in the areola of humans) that deeply penetrate the papillary dermis. These ridges may represent a morphological adaption to the nipple/teat’s attrition during suckling (Montagna, 1970; Mahler et al., 2004; Koyama et al., 2013). Also, in horses Ludewing (1997) mentioned that *dermal papillae* end immediately below the stratum corneum, which confirms its presence in equine MG skin.

Furthermore, the presence of a smooth muscle sphincter (SMS) in the teat area was described in the equines (Hughes, 2020a), rodents (Barbosa et al., 2019), bovine (Nickerson & Akers, 2011; Khan et al., 2020), dogs (Sorenmo, 2010; Evans & Christensen, 2013; Zappulli et al.,2019), and humans (Montagna, 1970; Koyama et al., 2013; Cardiff et al.,2018). The contraction of smooth muscle fibres (SMF) are proposed to wrinkle the teat/areola, enhancing nipple projection (Montagna, 1970; Koyama et al., 2013; Cardiff et al.,2018; Barbosa et al., 2019). Moreover, SMF have particular importance in dairy cows to maintain the teat

canal tightly closed between milking, preventing leakage, and avoiding bacteria from progressing upward into the teat cistern in cows (Nickerson & Akers , 2011). Cow's teats with weak, relaxed, or incompetent circular smooth muscle bundles (sphincters) are termed 'patent' or 'leaky' (Nickerson & Akers , 2011; Khan et al., 2020).

### 2.2.2 Mammary gland parenchyma

For ease of understanding, the MG can be divided into two compartments: the epithelial (or parenchymal) and the stromal (or mesenchymal) compartments (Masso-Welch et al., 2000). The epithelial compartment comprises two primary cell types: the luminal epithelial cells (LEC) and the myoepithelial cells (MEC), with a basement membrane surrounding these epithelial components (Fig. 2) (Dusek et al., 2012; Cardiff et al., 2018; Biswas et al., 2022), as already described. Both these layers are in constant flux with new ductal growth (elongation and branching) emanating from medially located epithelial cells that penetrate through gaps between the MEC layer (Sorenmo, 2010).

These bilayer conformation is observed in the gland cistern, large and small ducts and alveoli of mice (Barbosa et al., 2019), cows (Alsodany & Al-Derawi, 2018), and goats (Pattison, 1952) MGs, contrasting with the teat canal squamous stratified epithelium.

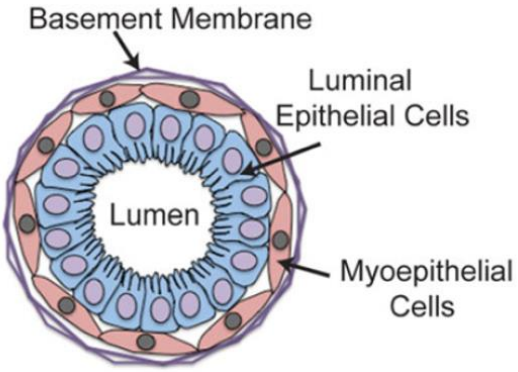


*Figure 2 - Schematic diagram of a mammary duct in cross-section (adapted from Dusek et al., 2012).*

#### 2.2.2.1 Luminal epithelial cells

The **luminal epithelium,** whose apical surface contacts the lumen of ducts, ductules, and alveoli forms the inner layer surrounding the hollow lumen

(Masso-Welch et al., 2000; Cardiff et al.,2018; Barbosa et al., 2019). In late pregnancy, responding to hormonal signals (Davis & Fenton, 2013; Zappulli et al., 2019), this layer becomes a functionally differentiated secretory epithelium responsible for milk synthesis and secretion during lactation (Masso-Welch et al., 2000; Cardiff et al.,2018). The LEC layer of the secretory alveoli differentiates into lactocytes, a cuboidal highly polarised cell, which ensures the movement of milk components toward the lumen. Also, fat vacuoles and Golgi vesicles containing lactose, milk proteins, and water may be seen on the lactocytes' cytoplasm (Masso-Welchet al., 2000; Davis & Fenton, 2013; Cardiff et al., 2018). The alveolar epithelium usually presents a spongy appearance during lactation, due to the intracellular lipid and osmotic swelling of lactose-containing secretory vesicles (Masso-Welch et al., 2000).

On the other hand, in horses (Hughes, 2020a), humans (Cardiff et al., 2018), mice (Masso-Welch et al., 2000; Davis & Fenton, 2013), dogs (Sorenmo, 2010; Zappulli et al. 2019), cows (Nickerson & Akers, 2011), and dromedaries (Kausar et al. 2001), the non-secretory alveoli resemble the small ducts with small LEC.

Not considering the physiological state of the gland, the existing literature on different animal species mentions variation from cuboidal to columnar appearance of the LEC (table 1).

*Table 1 – Different LEC appearances in gland cistern/lactiferous sinus, duct/ductules and alveoli, documented in humans, mice, dogs, and cows.*

| | ***Humans*** | ***Mice*** | ***Dogs*** | ***Cows*** |
|---|---|---|---|---|
| ***Gland Cistern /Lactiferous Sinus*** | **tall columnar** (Cardiff R. et al.,2018) | 1) **bilayered cuboidal to columnar** (Masso-Welch P. et al., 2000)<br>2) **columnar** (Davis B. & Fenton S., 2013) | **cuboidal to columnar** (Zappulli et al. 2019) | **more columnar** than cuboidal (Nickerson and Akers, 2011) |
| ***Ducts and Ductules*** | **cuboidal or columnar** (Cardiff R. et al.,2018) | **cuboidal or columnar** (Masso-Welch P. et al., 2000) | **cuboidal** (Sorenmo K., 2010) | |
| ***Alveoli*** | **cuboidal** (Cardiff R. et al.,2018) | **cuboidal to columnar** (Davis B. & Fenton S., 2013) | **cuboidal to columnar** (Sorenmo K., 2010) | **cuboidal to columnar** (Davis B. & Fenton S., 2013) |

#### 2.2.2.2 Myoepithelial cells

The MEC layer is located between the alveolar secretory epithelium and the basement membrane. There is increasing evidence that these cells have multiple functions (e.g., mammary morphogenesis), influencing the proliferation, survival, and differentiation of LEC and the structural formation of the ducts, and milk expulsion from the alveoli to the teat (Nickerson & Akers, 2011; Davis & Fenton, 2013). The milk ejection is activated by oxytocin, that binds to MEC receptors and stimulates intracellular calcium signalling, resulting in MEC contraction (Hassiotou & Geddes, 2012; Líška et al., 2016; Cardiff et al., 2018; Hughes, 2020a).

Furthermore, MEC undergo some changes throughout the reproductive cycle (Davis & Fenton, 2013; Zappulli et al., 2019; Cardiff et al., 2018). It assumes a more fusiform shape during lactation due to the stretching resulting from the luminal high pressure caused by the presence of milk. This was described in mice (Masso-Welch et al., 2000) and dogs (Sorenmo, 2010). In contrast, in the proliferative state, MEC are called “hypertrophic” and are easily identified by their polygonal shape with vacuolated cytoplasm and ovoid nucleus, in dogs (Espinosa de los Monteros et al.,2002; Zappulli et al., 2019; Łopuszyński et al., 2019).

In dog’s gland cistern, MEC tend to be more columnar and cuboidal compared to the MEC of ducts and alveoli (Zappulli et al., 2019).

### 2.2.3 Mammary gland stroma

The MG consists of epithelial glandular tissue and connective tissue (Evans & Christensen, 2013). The connective tissue may be subdivided into two components: the **intralobular stroma (IAS)**, embedding the alveoli; and the **interlobular stroma (IES)**, a “far stroma” equivalent that creates an artefactual space around the TDLU (Hughes, 2020a; Cardiff et al., 2018; Biswas et al., 2022). In equines and ruminants, the IAS consists of a densely packed collagenous and highly cellular stroma, while IES is looser and sparsely cellular (Hughes, 2020a). In contrast, in dogs and humans, the IAS looser stroma is arranged in fine collagen fibres within an extensive extracellular matrix (Zappulli et al., 2019;

Cardiff et al.,2018). In addition, blood vessels, nerves, and lymphatics vessels may also be found in the IES of canine MGs (Zappulli et al., 2019).

The connective tissue stroma differs in thickness, composition, and density throughout the oestrous cycle. During pregnancy, lobules expand and are filled with secretion; consequently, the IES turns out more collagenous and elastic to adjust and agglomerate all the hypertrophic lobules, protecting the delicate synthetic tissues during ductal elongation and branching (Nickerson & Akers, 2011; Biswas et al., 2022). Some authors mentioned a decrease in thickness of the extra- and intra-lobular stroma during pregnancy in mice (Masso-Welch et al., 2000; Davis & Fenton, 2013; LÍŠKA et al., 2016).

In addition, in non-lactating canine MG, IES is described as more abundant and compact compared to the IES of the active MG (Sorenmo, 2010; Davis & Fenton, 2013). Studies in mice mentioned a relative depletion of fibrous collagenous stroma at the end of the lactating period, due to the replacement of glandular secretory component with adipose and connective tissue (Masso-Welchet al., 2000; Davis & Fenton, 2013; Líška et al., 2016; Cardiff et al., 2018). Moreover, Kausar et al. (2001) stated that, in dromedaries, the MGs parenchyma is replaced by loose connective tissue over mammary involution.

## 3. Mammary gland development

The prenatal MG development begins usually during the first third of pregnancy (McGeady et al., 2006) the MGs undergo allometric growth in proportion to the rest of the body (Sorenmo, 2010; Watson & Walid, 2020; Biswas et al., 2022). Dual primary sprouts emerge initially from the epidermis due to the proliferation of teats' epithelium, forming secondary sprouting of mammary and pilosebaceous outgrowths (Hovey & Trott, 2004; McGeady et al., 2006; Hurley et al., 2011; Watson & Walid, 2020; Biswas et al., 2022). The ramification of these sprouts results in two independent teat cisterns and mammary trees. Each sprout will form a mammo-pilo-sebaceous unit (MPSU) composed of a hair follicle, a sebaceous gland, and a mammary ductal system, which will be retained in mature mares (Fig. 3) (Hughes, 2020a). Kausar et al. (2001) stated that, also in dromedaries, the follicles are associated with sebaceous glands, although not

using the “MPSU” term. In cats, MPSU could only be seen in immature domestic animals until approximately one week after birth, but this structure regresses by three months of age (Hughes, 2020a).

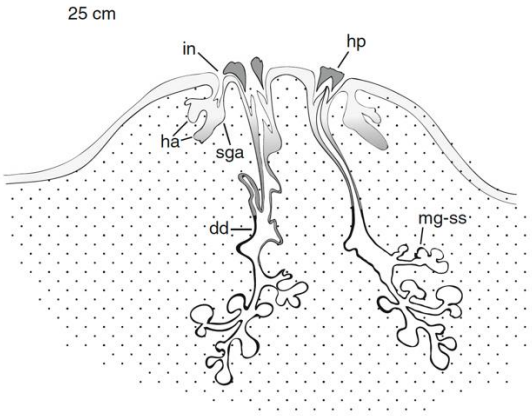


*Figure 3 - Schematic representation of Equus caballus MG at around 150 days of pregnancy: in - infundibula of hair follicles, ha- hair anlagen, sga- sebaceous gland anlagen, dd- distended ducts, hp- horny plugs in the opening of a streak canal, mg-ss- ramification of secondary sprouts (Oftedal and Dhouailly, 2013).*

During the embryonic development, the primitive germ layers, ectoderm, and mesoderm originate the epithelial (luminal and myoepithelial cells) and mesenchymal (stromal cells) compartments (Oftedal and Dhouailly, 2013). Studies in dogs (Davis & Fenton, 2013) and mice (Masso-Welch et al., 2000) evidenced that the postnatal period is marked by active cellular proliferation, matrix remodelling, and epithelial invasion. At microscopic analysis, the samples show essentially ductal structures (a main lactiferous duct with secondary ducts) (Barbosa, 2019).

The terminal end bud (TEB) is the growing end of the mammary tree, commonly observed in sections of MG of young mice (Hughes & Rudland, 1990; Líška et al., 2016; Cardiff et al., 2018; Barbosa et al., 2019), humans (Hassiotou & Geddes, 2012; Biswas et al., 2022), dogs (Leeuwen et al., 2000), and cows (Nielsen et al., 2011). The TEB is a solid or semisolid bulbous club-like structure of immature epithelial cells (Russo, 1978), that should not be confused with a hyperplasia focus. It has two morphologically distinct cellular compartments (Fig. 4): (1) an inner and central layer of body cells, with a high apoptotic index that will give rise to the future ductal and alveolar LEC (Humphreys et al., 1996; Biswas et al., 2022); and (2) the outer compartment of a highly proliferative single-

cell layer of “cap cells” that surrounds the “body cells” (Daniel & Smith, 1999). In mice, the significant components of stromal connective tissue that support the development of TEBs are adipocytes, fibroblasts, nerves, vascular endothelial cells, and a variety of innate immune cells, such as macrophages, mast cells, and eosinophils that escort the growing end (Cardiff et al.,2018; Biswas *et al.*, 2022).

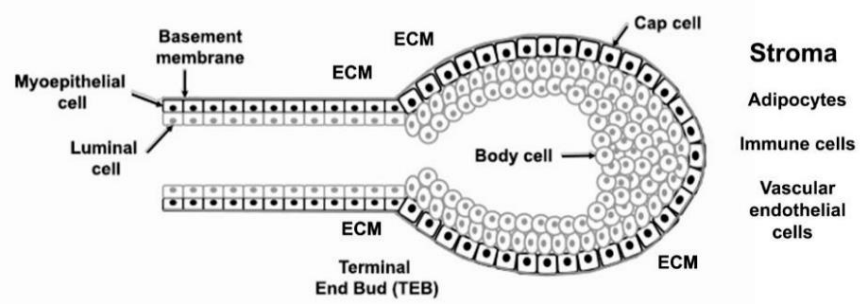


*Figure 4 - Schematic representation of a terminal end bud (TEB) (Biswas et al., 2022).*

Jennies start cycling regularly between 10 and 22 months old, with the ability to reproduce at one and a half years old (Quaresma, 2005; Quaresma & Nóvoa, 2018). In response to sex hormones, the “body cells” from TEBs differentiate in cells from the ductal lumina, and “cap cells” give rise to both MEC and basement membrane (a reservoir of mammary stem cells with regenerative properties) (Masso-Welch et al., 2000; Bai & Rohrschneider, 2010; Hassiotou & Geddes, 2012; Davis & Fenton, 2013; Rios et al., 2014; Líška et al., 2016; Biswas et al., 2022). The epithelial tree undergoes exponential growth and branches into lobes and lobules to fill the entire mammary parenchyma (Davis & Fenton, 2013; Yallowitz et al. 2014). Stromal components such as fibrillar collagens type I, III, and IV, that are in direct contact with TEBs, regulate IAS and IES composition and function (Biswas *et al.*, 2022). Additionally, over multiple oestrous cycles, the lobules accumulate progressively (Masso-Welch et al., 2000; Barbosa et al., 2019).

## 4. Reproductive cycle and mammary gland histological changes

The MG responds to the surges in hormones associated with ovulation and luteinization with increased mitotic activity. Pregnancy is associated with MG

enlargement and cell proliferation as the TDLU grows and acini develop and matures. Toward the end of pregnancy and during lactation, cell proliferation slows and further MG enlargement results from alveolar hypertrophy (Cardiff et al.,2018).

In species with a **menstrual cycle**, such as human and non-human primates, oestrogens are essential for duct development, while progesterone and oestrogen, along with prolactin, drive the lobuloalveolar proliferation during pregnancy (Davis & Fenton, 2013). Consequently, in these species an increased mitotic activity is essentially detected during the luteal phase (Cardiff et al., 2018). On the other hand, in non-primate species with an **oestrous cycle**, that have longer oestrogen- or progesterone-influenced stages, MG morphology can vary dramatically from a ductular proliferative state in prooestrus and oestrus to an alveolar secretory state in dioestrus (Davis & Fenton, 2013). In dogs, the best ductal proliferation occurs during the luteal phase, but alveolar proliferation is essentially potentialized in the follicular phase (Davis & Fenton, 2013). Sorenmo (2010), Davis & Fenton (2013) e Zappulli et al. (2019), also in dogs, mentioned a greater development of the ducts with the formation of lobules occurs in this stage of the cycle. On the contrary, in mice the increased mitotic activity usually occurs during oestrus. (Cardiff et al., 2018) and metoestrus (Líška et al., 2016).

## 5. Immunohistochemistry and immunohistochemical markers

Immunohistochemistry is an integral technique in many veterinary laboratories for diagnostic and research purposes. This technique is based on the binding of antibodies (Abs) to a specific antigen (Ag) in tissue sections. Once antigen–antibody (Ag-Ab) binding occurs, the complexes are evidenced with a coloured histochemical reaction visible by light microscopy (Ramos-Vara, 2005).

The **AE1/AE3** monoclonal antibody, also called **pancytokeratin,** is a combination of 2 monoclones, AE1 and AE3, both of which recognize a wide spectrum of cytokeratins that form the cytoskeleton of epithelial cells (Bussolati et al., 1986; Toniti et al., 2010), staining its cytoplasm (Gartner et al., 1999; Gama et al., 2003; Toniti et al., 2010; Brocca et al., 2020). AE1/AE3 is a good marker for epithelial cells in the normal MG and mammary tumours in dogs (Vos et al,

1993a; 1993b; 1993c; Griffey et al., 1993; Gartner et al., 1999; Zuccari et al., 2002; Toniti et al., 2010).

**α smooth muscle actin** (α-SMA) is a contractile protein mainly found in cells having contractile functions and is a valuable marker for studying the differentiation process of smooth muscle cells (SMC) in normal and pathological conditions (Gugliotta et al., 1988; Marettová & Maretta, 2018). α-SMA has been long used as a phenotypic marker for identifying mammary MEC quantitatively in humans (Gugliotta et al., 1988; Deugnier et al., 1995), bovines (Hellmén & Isaksson, 1997; Alkafafy et al., 2012; Marettová & Maretta, 2018) and equines (Spaas at al. 2012; Hughes, 2020a), since a large amount of actin in microfilament bundles contrasts with the relatively low content of filamentous actin in LEC. Apart from MEC, the SMC of the blood vessels and pericytes of the capillaries also reveal a strong immunostaining reaction for SMA, in addition to stromal myofibroblasts (Marettová & Maretta, 2018).

**Calponin** (CALP) is a specific 34-kDa protein involved in the regulation of SMC contraction, which expresses diffuse cytoplasmic staining in MEC (Łopuszyński et al., 2019). However, like α-SMA, its value as a marker for MEC is limited by the fact that it also labels stromal myofibroblasts and vascular SMC (Espinosa de los Monteros et al., 2002; Moritoni et al., 2002; Sánchez-Céspedes et al., 2013; Łopuszyński et al., 2019). The high sensitivity of calponin as a marker of MEC in the equine (Brocca et al., 2020), canine (Espinosa de los Monteros et al., 2002; Rasotto et al., 2014; Sorenmo K., 2010; Zappulli et al. 2019; Łopuszyński et al., 2019), feline (Espinosa de los Monteros et al., 2002), and human MG (Łopuszyński et al., 2019), as it was demonstrated in previous studies.

According to what was previously reported in mice (Yallowitz et al. 2014) humans (Gatti et al. 2019), and dogs (Ramalho et al. 2006; Toniti et al., 2010; Sorenmo, 2010; Łopuszyński et al. 2019), the **p63** antibody is a sensitive and highly specific marker displaying a nuclear staining pattern in the basal cell layer, that labels to myoepithelial and interspersed stem/progenitor cells along the ductal-acinar structures and the stratified epithelia of the skin. It shows a limited expression in LEC. The p63 protein is a product of the p63 gene translation,

crucial for sustaining the proliferative potential and self-renewing capacity of mammary epithelial stem cells (Ramalho et al., 2006; Gatti et al., 2019).

**Vimentin** is a cytoskeletal type III intermediate filament (IF) protein that forms part of the cytoskeleton of basal/myoepithelial cells and mesenchymal cells, such as fibroblasts/myofibroblasts, endothelial cells of blood vessels, macrophages, and lymphocytes and is essentially distributed in their cytoplasm (Coulombe & Wong, 2004; Peuhu et al., 2017; Battaglia et al., 2018; Marettová & Maretta, 2018; Barbosa et al., 2018). Consequently, vimentin antigen is widely used as a mesenchymal marker and displays a cytoplasmic staining pattern in dogs MG (Gartner et al., 1999; Gama et al., 2003; Toniti et al., 2010). Additionally, vimentin filaments also play an important role in mediating active force of smooth muscle fibres (Wang et al., 2006), since type III IF vimentin proteins and desmin are the major constituents of the IF networks in this cell type (Tang, 2008).

Given that commercial antibodies are most usually developed for use in human or murine tissues, it is vital that immunohistochemical studies follow rigorous protocols and that antibodies are tested and standardized when using them on other animal species tissues, including appropriate positive and negative controls.

In horses, there are some published studies using immunohistochemical markers in mammary gland tumors and healthy MG. α-SMA MEC expression has previously been demonstrated in normal equine MG (Hirayama et al., 2003; Hughes, 2020a). Scarce information exists on the normal pattern of expression of the abovementioned markers in equids, the existing information available focusing in their expression in mammary lesions. The expression of intermediate filaments has been assessed in a few number of equine mammary carcinomas; according to the published results, carcinomas showed a heterogeneous expression, with tumour cells expressing CK AE1AE3 and vimentin, with varying degrees of intensity (Hirayama et al., 2003; Laus et al., 2009; Gamba et al, 2011; Hughes et al., 2015; Bussche et al., 2017; Júnior et al., 2019; Sabiza et al., 2020; Brocca et al., 2020). Reesink et al. (2009) also used CK AE1AE3 and vimentin in horse mammary gland to test a malignant fibrous histiocytoma, that stained positive for vimentin and negative for CK AE1AE3. Positive staining for α-SMA (Bussche et al., 2017; Reesink et al., 2009) and calponin (Brocca et al., 2020)

has also been reported in mare mammary tumours. Also, Hirayama et al., 2003, tested calponin and α-SMA in invasive ductal mammary carcinoma, with negative results.

The immunohistochemistry is a crucial technique in the characterization of the morphometry of the mammary gland, as it allows to distinguish between the different cell types and accentuate the cells morphologic features when a suitable set of primary antibodies is used.

## II. Aims

The aims of this study were the following:

1. Characterize the anatomic and histomorphological features of BMB donkeys' mammary glands;
2. Characterize BMB donkeys' mammary glands by immunohistochemistry, with the optimization of this technique to donkeys' mammary tissue;
3. Compare donkey's mammary gland histology with other animal species;
4. Investigate the presence of MG alterations, including proliferative lesions.

## III - Materials and Methods

### 1. Samples

Sixty-five mammary gland tissue samples were obtained from BMB jennets (*Equus asinus)* guarded by AEPGA between 2009 and 2018 (9 years). After the animals' natural death, the samples were collected, fixed in 10% neutral buffered formalin, and sent to the Laboratory of Histology and Anatomical Pathology (LHAP) at the Universidade de Trás-os-Montes and Alto Douro (UTAD), Portugal. Most of the analysed samples (n=58; 89,2%) corresponded to animals older than one and a half years old, the puberty age of jennets. Seven (n=7; 11,8%) prepubertal MG were identified, with four samples corresponding to newborn animals (up to 72h after birth). Multiple MG sections were made, from the teat (longitudinal sections) and the deepest mammary parenchyma. All samples in this study were examined by light microscopy and a routine haematoxylin and eosin staining; furthermore, sixteen samples were analyzed by immunohistochemistry, using five different markers. The sixteen samples were selected based on the age of the animals and the year in which the samples were collected. Table 2 groups the samples according to these criteria.

*Table 2 – Animal's age and year of collection of the sixteen samples chosen for the indirect immunohistochemistry technique. Y-years; M- Months*

| Animal's Age | | Year of the collection | Nº of samples |
|---|---|---|---|
| **<72h after birth** | | 2010 | 1 |
| **>72h after birth ≤18M** | | 2013 | 1 |
| **>18M and <10Y** | | 2011 | 2 |
| **> 18M** | **Lactating Gland** | 2010 | 3 |
| | | 2012 | 1 |
| | | 2016 | 1 |
| | | 2017 | 1 |
| | **Non-lactating Gland** | 2010 | 3 |
| | | 2011 | 1 |
| | | 2017 | 2 |

In addition, the macroscopical anatomic features of the udders were analyzed *in vivo* and descried in detail.

## 2. Methods

### 2.1 Histology

After fixation, tissue sections were routinely processed for light microscopy. Tissues were progressively dehydrated in a series of alcohols, diaphanized with xylol and embedded in paraffin. Subsequently, paraffin blocks were cut at 3µm thick sections and automatically stained with haematoxylin and eosin (H&E) (*Thermo Electron Corporation Shandon Varistain 24-4)* for histopathological evaluation. Morphological alterations, including proliferative lesions, the presence of psammoma bodies, inflammatory cell infiltrate was recorded.

### 2.2 Immunohistochemistry

Paraffin-embedded tissue samples were cut in 3µm-sections on silanized slides, and used to perform the immunohistochemical analyses, by using the primary antibodies displayed in Table 3. The detection system applied was a polymeric labelling methodology (Novolink Polymer Detection System, Novocastra, UK), following the manufacturer's instructions. The immunohistochemical protocol consisted in the following steps:

1. The tissue samples were first dewaxed in xylol for 30 minutes, before being rehydrated through a series of graded alcohols (100%, 95%, 80%, and 70%).
2. The retrieval of antigens involved placing the samples in a suitable holder together with citrate buffer pH6 (Dako Target Retrieval Solution), without any prior heating. The holder was then microwaved for 5-minute cycles at 750W, with the number of cycles adjusted depending on the primary antibody used (Table 3). If more than one cycle was necessary, retrieval solution was replenished after each cycle to prevent dehydration of the samples.
3. The supplier technique proved to be challenging in this animal species tissues when it came to enzyme blockade and protein blockade. To overcome this problem, the exposure time to 3% hydrogen peroxide ($H_2O_2$) was increased from 5 to 45 minutes to block the endogenous peroxidase activity. Afterward, the samples were washed with phosphate buffer saline (PBS) at pH 7.6, three times.

4. To reduce non-specific background labelling, the incubation time of ***Novocastra Protein Block*** (Leica Biosystems, Newcastle, United Kingdom) was also increased from 5 to 7 minutes. This is a serum-free casein-based blocker. Additionally, the primary antibody immediately without washing with PBS. This further reinforced the blockage of endogenous protein.
5. Excess reagent was removed and replaced by the primary antibodies and incubated at 4˚C, overnight, at specific dilutions: **AE1/AE3** (1:200, Monoclonal mouse anti-human, Dako®)**, vimentin** (1:100, Monoclonal mouse anti-vimentin, Novocastra®)**, p63** (1:100, Monoclonal mouse anti-p63, Abcam®735)**, α-smooth muscle actin** (1:50, Monoclonal mouse anti- α-SMA, Novocastra®) and **calponin** (1:400, Monoclonal Mouse Anti-Human Calponin, Dako®). Primary antibodies were diluted in PBS. Details of the primary antibodies used in this study are summarised in Table 3.
6. On the next day, after rinsing the slides three times with PBS, the sections were incubated with the secondary antibody ***Novocastra Post Primary*** (Rabbit anti-Mouse IgG, Leica Biosystems, Newcastle, United Kingdom) for 30 minutes; after rinsing the slides three times with PBS, sections were incubated with ***Novolink Polymer*** (anti-rabbit Poly-HRP-IgG; Leica Biosystems, Newcastle, United Kingdom) for 30 minutes, which recognize the rabbit immunoglobulins, detecting the *post-primary* and any tissue-bound rabbit primary antibodies.
7. After rinsing the slides with PBS, the colour was developed with the chromogen 3-3'-diaminobenzidine tetrahydrochloride (DAB) with 0,036% $H_2O_2$ in phosphate-buffered saline (PBS) for 5 minutes.
8. After rinsing the slides with PBS, slides were counterstained with Gill's Haematoxylin for 3 minutes, rinsed twice with tap water for 5 minutes, dehydrated in a series of ethanol (95%, 95%, 100%, and 100%), diaphanized with xylol and mounted with Entellan®.

*Table 3 - Antibodies used for immunohistochemical examination of JMG.*

| Antibody | Clone/Manufacturer | Dilution | Localization | Antigen retrieval | Species | Source of antibody |
|---|---|---|---|---|---|---|
| **CK AE1AE3** | AE1AE3/ Dako® | 1:200 | Cytoplasm | Microwave 750W, 1 cycle, 5 min | Monoclonal mouse anti-human | Santa Clara, California, USA |
| **Vimentin** | V9/Novocastra® | 1:100 | Cytoplasm | Microwave 750W, 1 cycle, 5 min | Monoclonal mouse anti-vimentin | Leica Biosystems, Newcastle, United Kingdom |
| **P63** | BC4A4/ Abcam® | 1:100 | Nucleus | Microwave 750W, 3 cycles, 5 min each | Monoclonal mouse anti-p63 | Cambridge, United Kingdom |
| **α-SMA** | alpha sm-1/ Novocastra® | 1:50 | Cytoplasm | Microwave 750W, 3 cycles, 5 min each | Monoclonal mouse anti-α-SMA | Leica Biosystems, Newcastle, United Kingdom |
| **Calponin** | CALP/Dako® | 1:400 | Cytoplasm | Microwave 750W, 3 cycles, 5 min each | Monoclonal Mouse Anti-Human Calponin | Carpinteria, California, USA |

### 2.2.1 Immunohistochemical evaluation

The immunohistochemical expression of the five markers used was semi-qualitatively evaluated. Positivity was indicated by the presence of distinct brown nuclear (p63) or cytoplasmic (CK AE1AE3, Vimentin, α-SMA, and calponin) staining. Epidermis was used as an internal positive control for p63 and CK AE1AE3 markers (*stratum basale* for p63); blood vessels, the basal myoepithelial layer of skin sweat glands and arrector pili muscle were used as internal positive controls for α-SMA and calponin; blood vessels and arrector pili muscle were also used as vimentin positive control (Table 4). As negative controls, PBS was used in place of the primary antibody in the standardized technique, to mitigate potential biases.

*Table 4 - Positive Control for each immunohistochemical marker.*

| Skin Structures | CK AE1/AE3 | α-SMA | P63 | VIM | CALP |
|---|---|---|---|---|---|
| Stratum Basale of the Epidermis | + | - | + | - | - |
| Hair Follicle Epithelial Sheath | + | - | + | - | - |
| Hair Bulb | + | - | + | - | - |
| Arrector Pili Muscle | - | + | - | + | + |
| Sweat Glands' Myoepithelial Layer | - | + | - | + | + |
| Blood Vessels | - | + | - | + | + |

## 3. Analysis

A descriptive analysis was performed, based on Microsoft Excel data analysis, and the results were expressed in absolute and relative frequencies.

## IV - Results

### 1. Macroscopic evaluation of jennet's mammary gland

Jennies' udder comprised one pair of teats, each with two orifices. The number of hairs observed on the teats was minimal. The udder's skin was dark brown. The teat skin was slightly thicker than the epidermis of the adjacent skin. Regarding teats shape and size, it varied from cylindrical to conical. Udders from animals that have already given birth or are in a lactational state showed larger teats and bigger and convex udders (Fig. 5), while young nulliparous animals exhibited small teats and udders (Fig. 6). Teats of non-lactating adult MGs remained large and elongated.

*Figure 5 - External appearance of BMB jennet's udder and teats. Caudal view of a convex udder with large and elongated teats.*

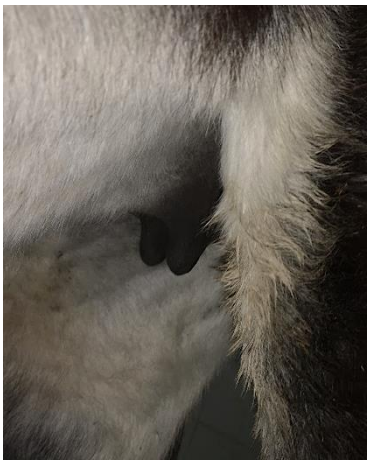

*Figure 6 - External appearance of BMB jennet's udder and teats. Lateral view of a small udder and less developed teats.*

### 2. Histological evaluation of jennet's mammary gland

#### 2.1 Mammary gland normal structure

##### 2.1.1Teat

The keratinized stratified squamous epithelium of the teat skin increases in thickness towards the teat orifices, with an increase of dermal papillae and epidermal ridges in this area (Fig. 7). Histologically, an increase of dermal papillae and epidermal ridges at the teat orifices area were observed (Fig. 7). An increased number of **melanocytes**, often with vacuolated cytoplasm, were found in the *stratum basale,* between the basal epidermal keratinocytes. The **dermis** is formed of networks of collagen and circular smooth muscle fibres (a circular

smooth muscle sphincter is present along the teat canal), blood vessels, and nerve fibres. Regarding the adnexal structures, these were non-existent at the entrance to the teat, in contrast with the epidermal extension of the teat towards the udder, which shows larger and individualized adnexal glands, although reduced in number (Fig. 8). The main duct, or the galactophorous duct, is part of a complex called the mammo-lobular-pilo-sebaceous unit (**MPSU**), which also embodies a hair follicle and a sebaceous gland (Fig. 7). This complex was observed in both immature and mature MG.

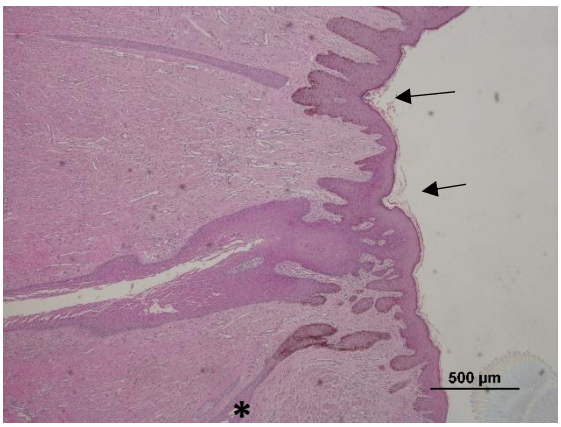


*Figure 7 - Donkey teat orifices: two ductal systems openings (arrows) with the respective sebaceous glands (*). No adnexa are observed in the dermis of the teat orifices. Notice the increased dermal papillae in this area. H&E stain. Scale bar= 500 µm.*

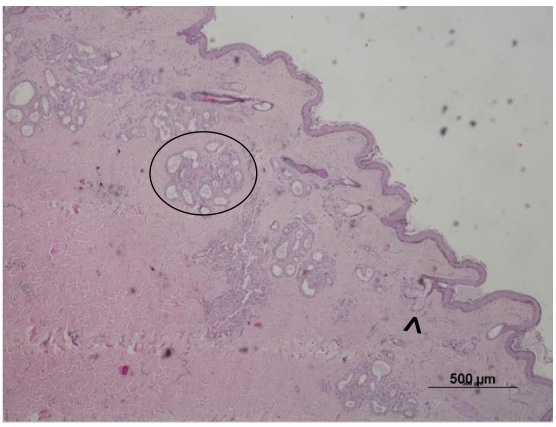


*Figure 8 - Donkey teat skin extension, with hair follicles and large sebaceous (arrowhead) and sweat (encircled) glands. H&E stain. Scale bar= 500 µm.*

In the analysed samples, the teat canal was lined by a stratified squamous epithelium that, at the entrance of the **gland cistern**, gradually changed from stratified to a bilayer epithelium, with an inner LEC and outer MEC layer (Fig. 9 and 10).

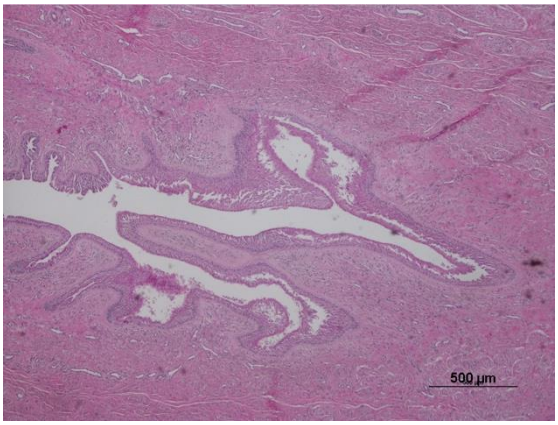


*Figure 9 - Donkey teat canals lined by stratified squamous epithelium with numerous smooth muscle trabeculae in the dermis around the teat duct. H&E stain. Scale bar= 500 µm.*

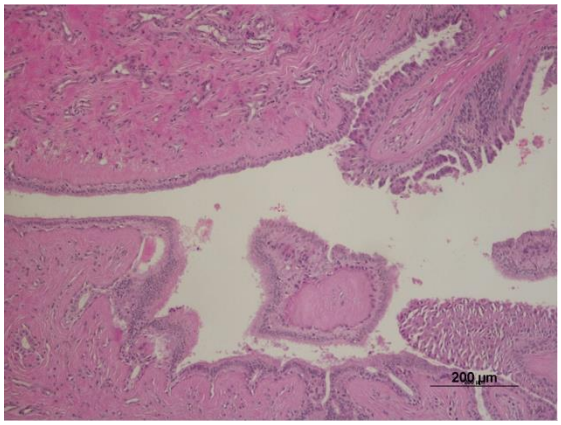


*Figure 10 - Donkey teat canal and gland cistern: the teat canal is lined by a stratified squamous epithelium that gradually changes to a bilayer cuboidal epithelium with peripheral myoepithelium, determining the gland/teat cistern region. H&E stain. Scale bar= 200 µm.*

### 2.1.2 Mammary parenchyma

In the analysed samples, LEC lining of the ducts and alveoli showed multiple shapes, such as cuboidal, columnar, or flattened, according to the MG's physiological state or the mammary region (more detail in "*immunohistochemical characterization of the donkey mammary gland: mammary parenchyma"* topic). In the proximal teat, the LEC tended to be more columnar than cuboidal, becoming more cuboidal near the alveoli. On the other hand, the secretory alveolar cells varied from pyramidal, cuboidal, or columnar before secretion to flattened after secretion, showing a variable number of intracytoplasmic lipid droplets that accumulate in the alveolar lumina, which makes the cytoplasm look foamy (Fig. 11). Nonetheless, the non-secretory alveoli are very similar to the small ducts.

The MEC shape varied from cuboidal to fusiform, assuming the most frequent cuboidal aspect in the teat area and the most fusiform to stellate shape in ductules and alveoli, usually showing pale-to-clear cytoplasm (Fig. 12).

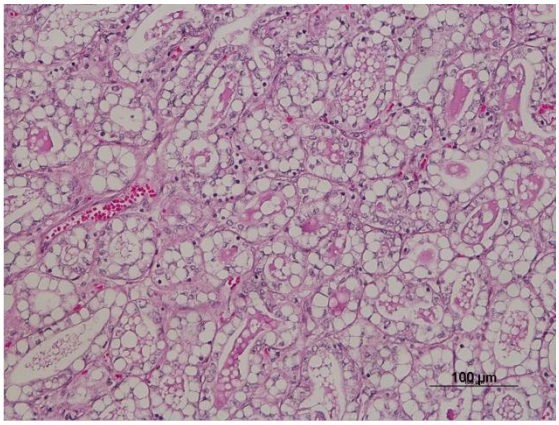


*Figure 11 - Donkey lactating MG with many secretory alveoli, containing lipid droplets in LEC cytoplasm. H&E stain. Scale bar = 100 µm.*

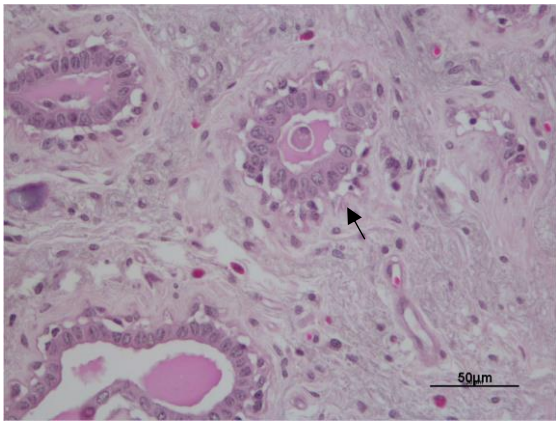


*Figure 12 – Donkey MG. The bilaminar arrangement of epithelial cells within the ductalveolar structures (arrow). Clear suprabasal MEC surrounding the cuboidal monolayer of LEC. H&E stain. Scale bar = 50 µm.*

### 2.1.3 Stroma

As expected, MG stroma was composed of connective and adipose tissue, blood vessels, lymphatics, and nerves, with variable number of inflammatory cells (see below). Surrounding the intralobular ducts, the **IAS** consisted of more cellular connective tissue, with intermingled undulated bundles of finer collagen fibres with a small amount of extracellular matrix. The **IES,** separating the lobules, consisted of denser and sparsely cellular connective tissue, with larger collagen bundles surrounded by a more extensive extracellular matrix (Figure 13).

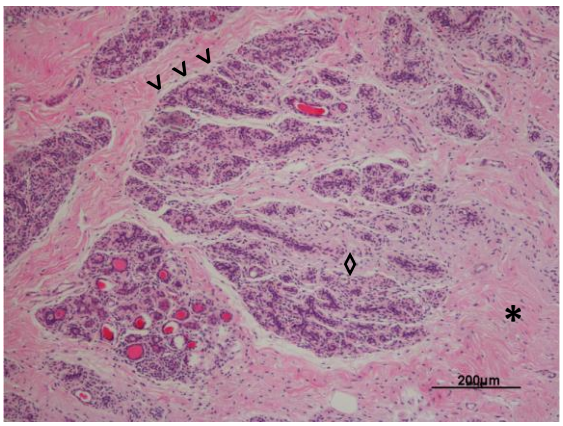


*Figure* 13 *– Donkey MG. The lobular arrangement of the mammary gland. Note the more cellular IAS (diamond) supporting TDLU's and the IES (*) surrounding the lobules. The border between the two stroma-types is well-demarcated in this image (arrowheads). H&E stain. Scale bar = 200 µm.*

## 2.2 Development of postnatal morphological changes in donkey mammary gland

Donkey MGs presented a structural organization, with two paired mammary complexes exhibiting distinct histological morphologies, from prepubertal (inactive/quiescent), to fully developed lactating and involuting MG.

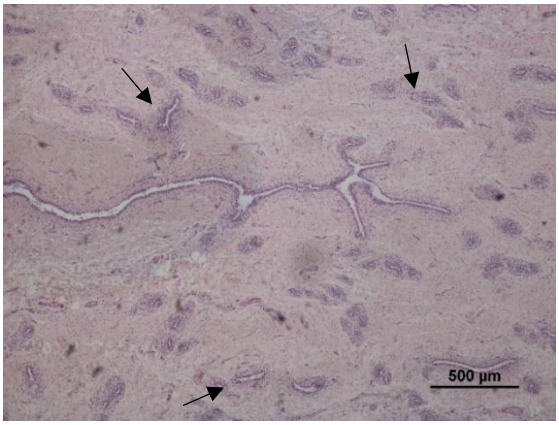


*Figure 14 - New-born donkey MG. Little ductal branching consists of primary ductal structures in small aggregates (arrows). H&E stain. Scale bar = 500 µm.*

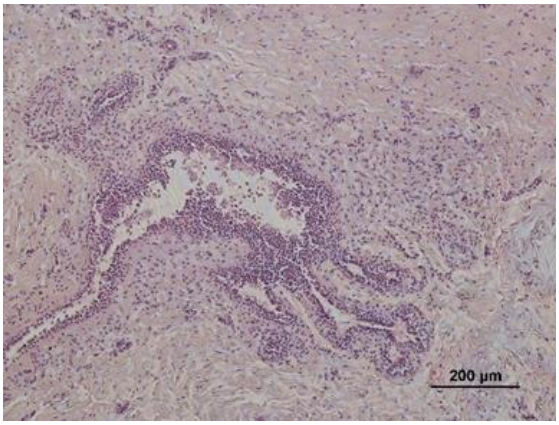


*Figure 15 - New-born donkey MG. Terminal end buds (TEBs), consisting of tightly packed multiple-layered cells. H&E stain. Scale bar = 200 µm.*

Although the number of newborn samples were not enough to withdraw unequivocal conclusions about the prenatal development of the MG, limited ductal branching was identified, consisting essentially of primary ductal structures in small aggregates (Fig. 14). In addition, terminal end buds (TEBs), bulbous epithelial structures comprised of tightly packed multiple-layered cells with large nuclei and indistinct cell borders, were also evident (Fig. 15).

The postnatal prepubertal MGs were inactive. Although revealing a better development of ductal structures than the neonatal samples, with relevant proliferation of IAS and IES, the mammary structures still showed a low degree of complexity and no evidence of previous lactational activity of the gland, such as the presence of PBs, lobular hyperplasia or luminal secretion.

In post-pubertal samples, morphological changes were observed in both the epithelial and stromal components, allowing the identification of different histological phases: lactating, non-lactating involuting MG, with intermedium phases.

Nineteen samples (29,2%) presented secretory lactational activity. Alveolar epithelial cells showed a variable morphology: in some specimens, LEC showed high cytoplasmatic lipid vacuolation, with no significant accumulation of lumen secretion (Fig. 16) while in other samples, LEC were regularly cuboidal, with no lipid cytoplasmatic droplets, and variable amounts of luminal secretion (Fig. 17). Moreover, alveoli and ducts showed a thin MEC layer that comprised fusiform cells (elongated-shaped cells).

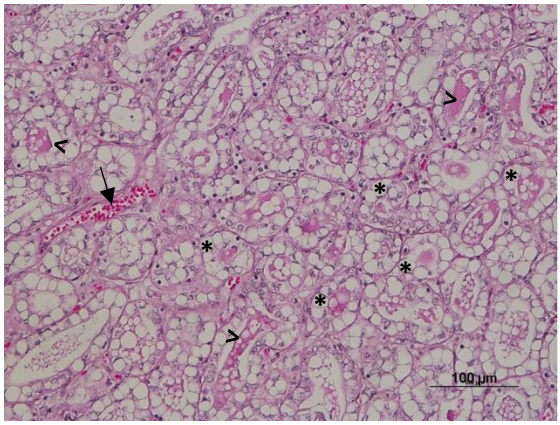


*Figure 16 - Donkey lactating MG. Alveolar LEC with intracytoplasmic lipid droplets (*) and pale staining of the cytoplasm. Notice the thin and attenuated layer of fusiform MEC. Little accumulation of secretion inside the alveolar lumen (arrowheads). Blood Vessel (arrow). H&E stain. Scale bar = 100 µm.*

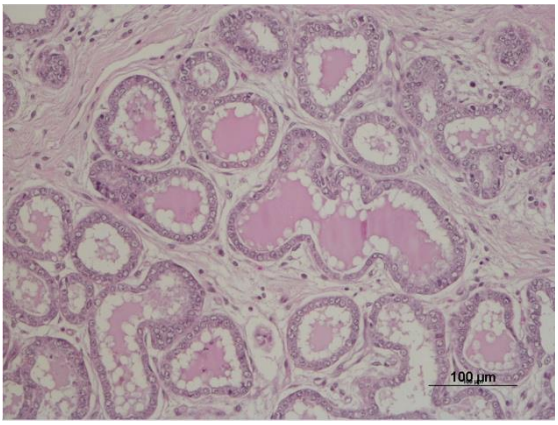


*Figure 17 - Donkey lactating MG. LEC are regularly cuboid, usually with centred nuclei, with few cytoplasmatic lipid droplets. The connective tissue surrounding the epithelial elements appears oedematous. H&E stain. Scale bar = 100 µm.*

Twelve (18,5%) samples were characterized by a non-lactational phenotype, with the presence of small lobules and alveoli, surrounded by a prominent mature interlobular and intralobular fibrous connective tissue (Fig. 18), and might correspond to post-lactational or senile involution. The ductules and acini were lined by small luminal and myoepithelial cells, very close to each other, with hyperchromatic nuclei and little cytoplasm (Fig. 19). Although the presence of eosinophilic luminal secretion was rare, focal ductal ectasia could be observed.

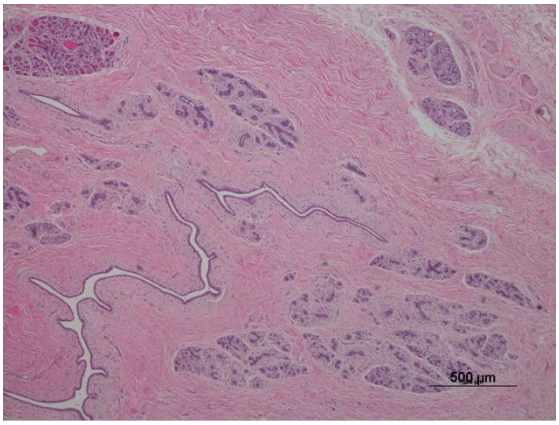


*Figure 18 - Donkey non-lactating MG. Well-defined ducts surrounded by fibrous IES. Presence of a reduced number of small and atrophic lobules. H&E stain. Scale bar = 500 µm.*

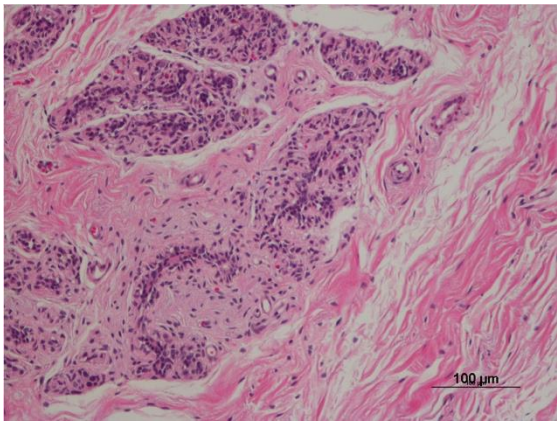


*Figure 19 - Donkey non-lactating MG. Atrophic glandular tissue with collapsed ducts, showing limited secretion. Luminal and myoepithelial cells are very close, and it is difficult to differentiate them. H&E stain. Scale bar = 100 µm.*

Twenty-seven (41,5%) samples showed intermediate or transitional morphologies between the lactational and non-lactational phenotype, probably corresponding to post-lactational mammary regression/involution. These MGs showed lobules of different sizes and a distinct morphology. Figs. 25 and 26 illustrate intermedium aspects of the MGs: Fig. 20 shows small inactive lobules and occasional hyperplastic lobules, with dilated ducts and alveoli, which could indicate a previous secretory activity; Fig. 21 shows hyperplastic lobules, characterized by ductal and alveolar collapse, with no luminal secretion.

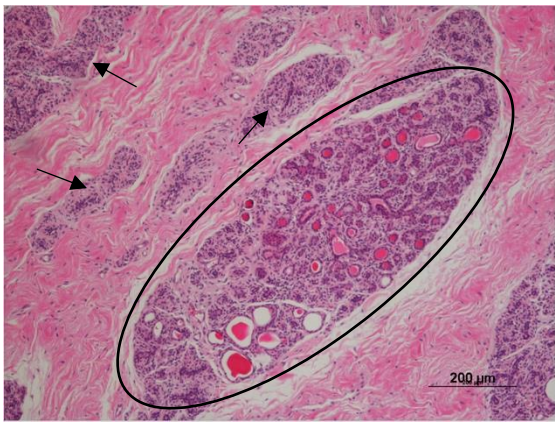


*Figure 20 - Donkey MG with transitional morphology. Hyperplastic secretory lobule (encircled) adjacent to inactive lobules (arrows). H&E stain. Scale bar = 200 µm.*

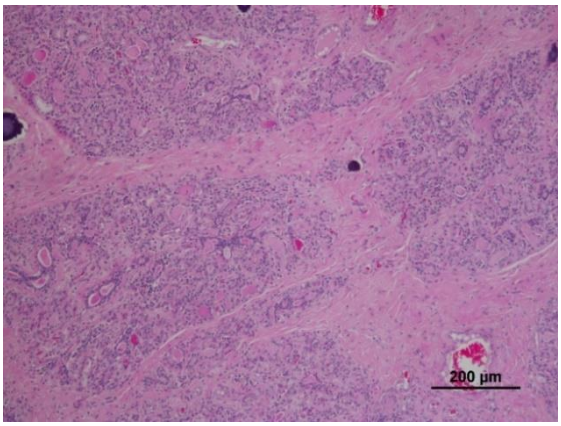


*Figure 21 - Donkey MG with transitional morphology. Hyperplastic lobules with an increased number of collapsed ducts and alveoli, with little secretion. H&E stain. Scale bar = 200 µm.*

## 3. Immunohistochemical characterization of the donkey mammary gland

### 3.1 Teat

The immunohistochemical markers used evidenced a differential expression across skin structures. The following table summarises the immunohistochemical results in teat samples.

*Table 5 – Differential expression of the immunohistochemical markers in teat skin structures.*

| **Skin structure** | **Immunohistochemical marker expression** |
|---|---|
| **Epidermis** | p63 – basal and suprabasal layers (Fig.22)<br>CK AE1AE3 – the entire epidermis (Fig.23) |
| **Hair follicles** | CK AE1AE3 (Fig.23) and p63 (Fig.22) - epithelial sheath and the hair bulb<br>α-SMA and calponin - arrector pili muscle (APM) (Fig.24) |
| **Sweat glands** | CK AE1AE3 - luminal cells (Fig. 23)<br>α-SMA (Fig.25), p63, vimentin, and calponin (Fig.24) - basal/myoepithelial cells |
| **Sebaceous glands** | CK AE1AE3 - epithelial cells (Fig. 23)<br>p63 - basal/myoepithelial cells (Fig.22) |

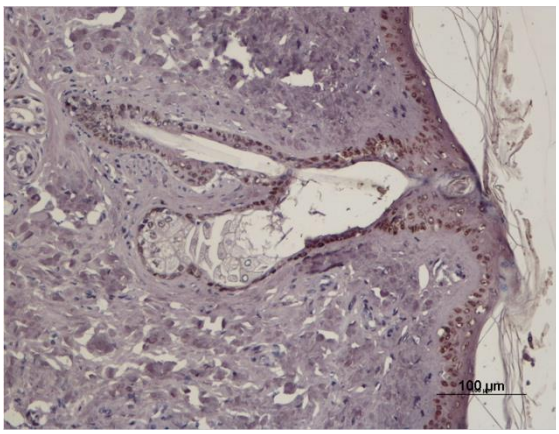


*Figure 22 - Donkey teat. p63 immunostaining. Nuclear expression in sheath, hair bulb epithelial cells, and basal epidermal and sebaceous epithelial cells. Haematoxylin counterstain. Scale Bar= 100 µm.*

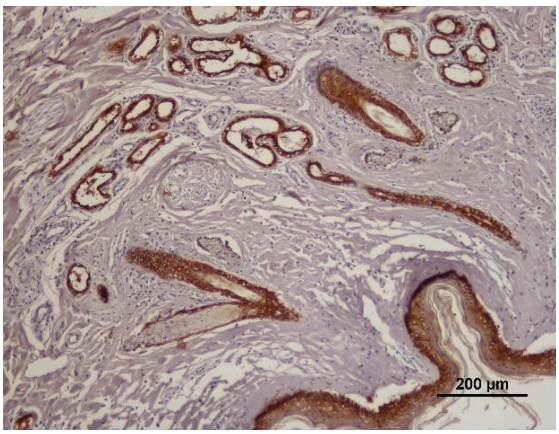


*Figure 23 - Donkey teat. CK AE1AE3 immunostaining. Intense expression in hair follicles and sweat glands (LEC layer) and moderate expression in sebaceous glands. Haematoxylin counterstain. Scale Bar= 200 µm.*

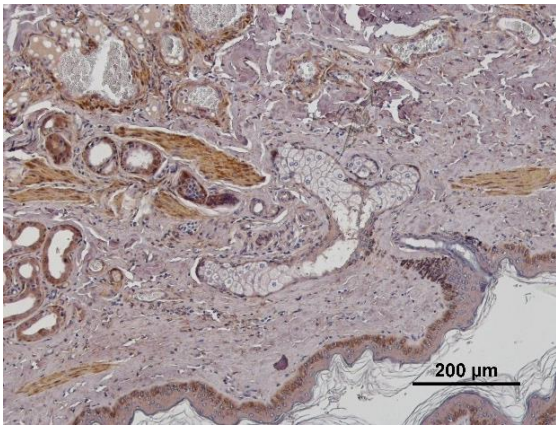


*Figure 24 - Donkey teat. Calponin immunostaining. Intense expression in APM, sweat glands MEC layer and blood vessels. Haematoxylin counterstain. Scale Bar= 200 µm.*

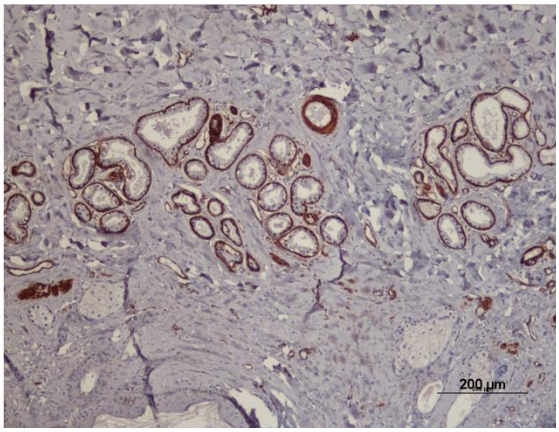


*Figure 25 - Donkey teat. α-SMA immunostaining. Intense expression in sweat glands MEC layer. Haematoxylin counterstain. Scale Bar= 200 µm.*

The cells in the gland cistern and small ducts assumed different affinities for the markers, clearly demarking the LEC and MEC layers. CK AE1AE3 was expressed by both epithelial cell layers: from the skin epidermis to the transitional bilayer epithelium, at the beginning of the gland cistern (Fig. 26 and 27). In the gland cistern and small ducts, p63 expression was found exclusively in the nuclei of MEC (Fig 28 and 29).

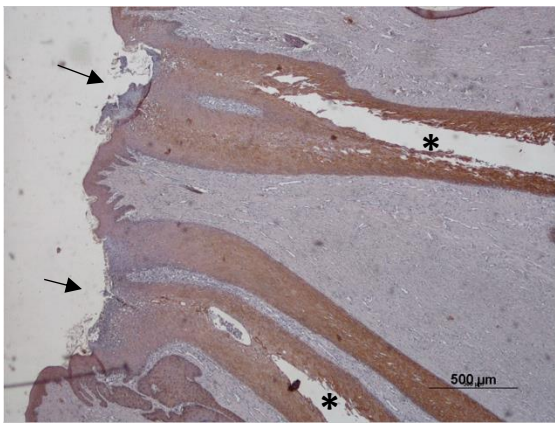


*Figure 26 - Donkey teat orifices and teat canals. CK AE1AE3 immunostaining. Two orifices (arrows) and the respective teat canals (*). Stratified squamous epithelium showing a moderate to strong CK AE1AE3 straining. Haematoxylin counterstain. Scale bar = 500 µm.*

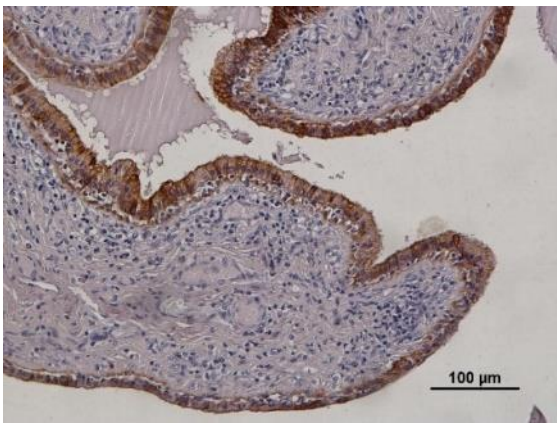


*Figure 27 - Donkey gland cistern. CK AE1AE3 immunostaining. Gland cistern: LEC intensely stained in contrast with the MEC layer, which show a moderate membrane expression. Haematoxylin counterstain. Scale bar = 100 µm.*

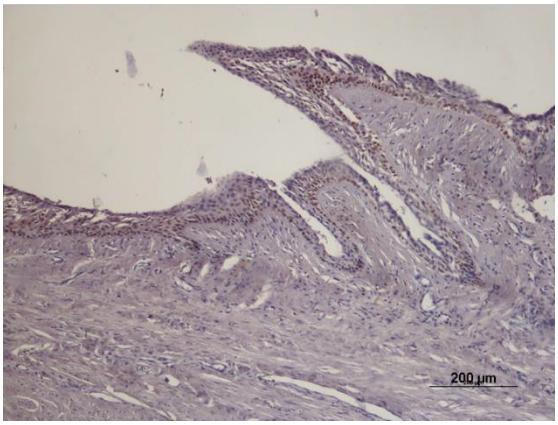


*Figure 28 - Donkey teat canal. p63 immunostaining. Basal epithelial layer expressing nuclear p63. Haematoxylin counterstain. Scale bar = 200 µm.*

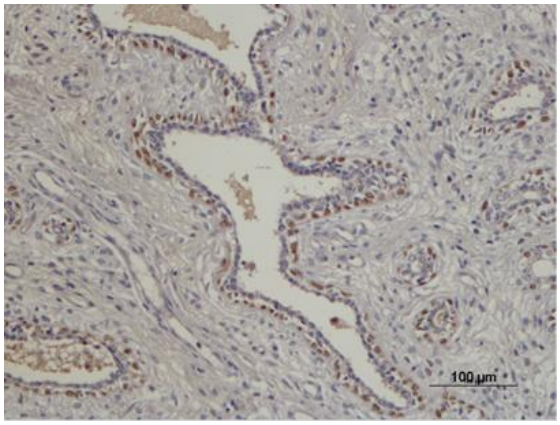


*Figure 29 - Donkey mammary parenchyma. p63 immunostaining. MEC nuclei of small ducts positive for p63. Haematoxylin counterstain. Scale bar = 100 µm.*

From the teat canal to the gland cistern, α-SMA and calponin showed an increasing affinity to the muscular component of MEC layer, evidencing a more intense positivity in the contours of the bilayer epithelium (Fig. 30). The large amount of actin in microfilament bundles of small ducts' MEC layer also expressed these makers (Fig. 30 and 31).

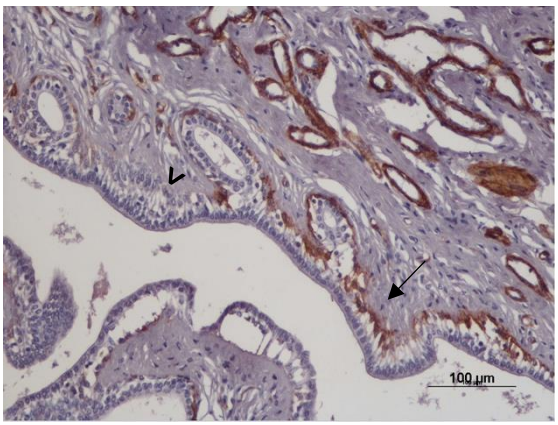


*Figure 30 - Donkey gland cistern. α-SMA immunostaining. Transitional region between the teat canal and the gland/teat cistern. α-SMA showed no expression on teat canal (arrowhead) in contrast with gland cistern, where the MEC epithelium is delimited (arrow). Haematoxylin counterstain. Scale Bar = 100 µm.*

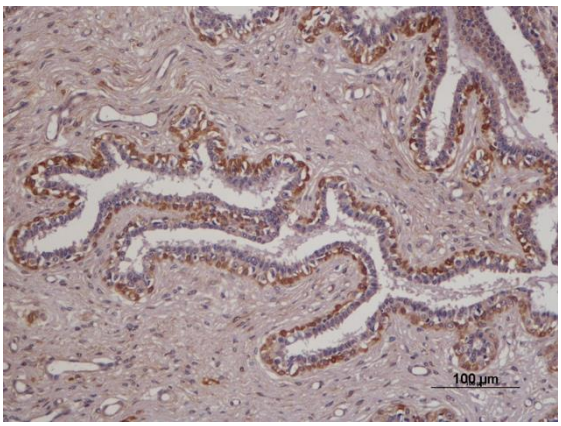


*Figure 31 - Donkey mammary parenchyma. Calponin immunostaining. Positive staining demarking MEC of small ducts. Haematoxylin counterstain. Scale bar = 100 µm.*

The SMS fibres stained against α-SMA, vimentin (Fig. 32), and calponin (Fig. 33), highlighting an inner muscular layer of longitudinal fibres and an outer muscular layer of transverse or circular fibres surrounding the teat canal.

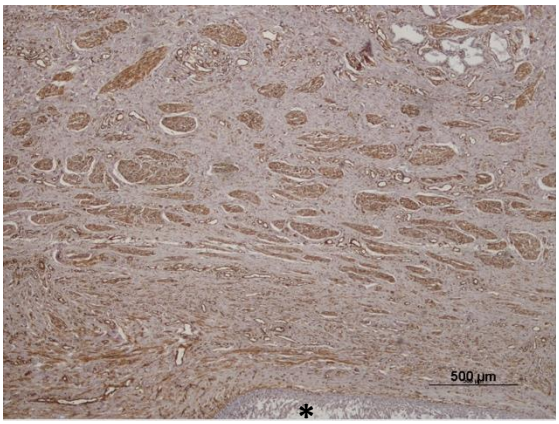


*Figure 32 – Donkey teat SMS. Vimentin immunostaining. Numerous prominent smooth muscle trabeculae surround the teat canal. Teat canal lumen (*). Haematoxylin counterstain. Scale bar = 500 µm.*

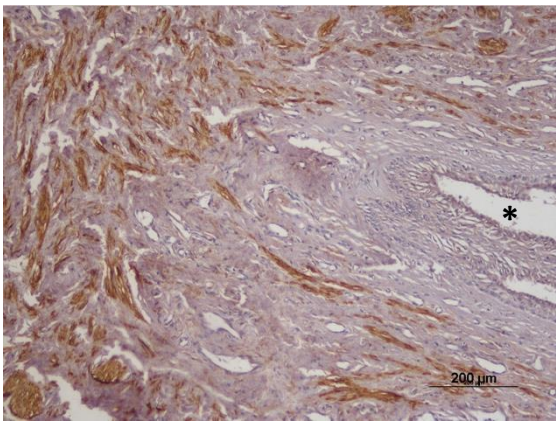


*Figure 33 – Donkey teat SMS. Calponin immunostaining. Smooth muscle intensely positive. Teat canal lumen (*). Haematoxylin counterstain. Scale Bar= 200 µm.*

## 3.2 Mammary parenchyma

The immunohistochemical markers highlighted the weak ductal branching in the new-born samples. In those samples, CK AE1AE3 (Fig. 34) and p63 (Fig. 35) stained both the body and cap cells of TEBs. Cap cells assume a stellate or vacuolated appearance, being also positive for α-SMA (Fig.36) and calponin. Vimentin showed that the IAS is less prominent than the IES (Fig. 37).

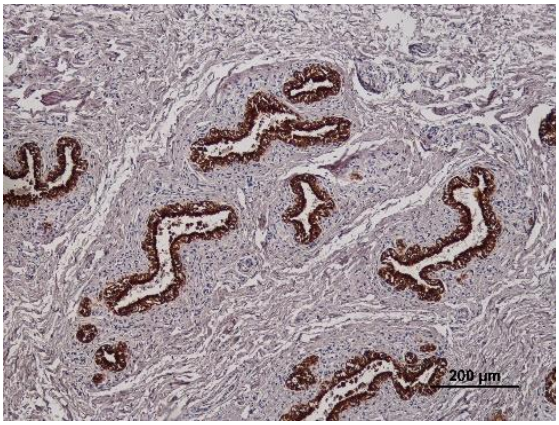


*Figure 34 – New-born donkey MG: TEBs. CK AE1AE3 Immunostaining. CK AE1AE3 stains both TEBs body and cap cells. Haematoxylin counterstain. Scale Bar= 200 µm*

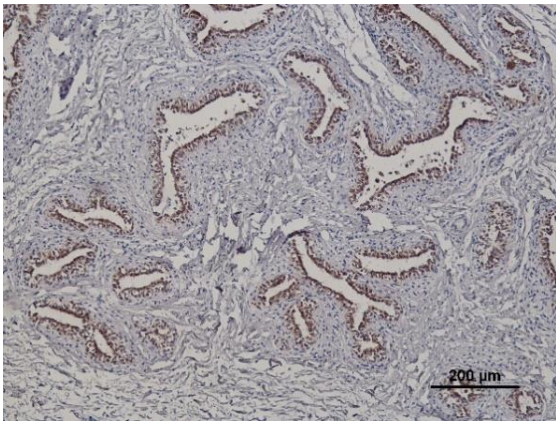


*Figure 35 – New-born donkey MG: TEBs. p63 immunostaining. The p63 is expressed in TEBs epithelial component. Haematoxylin counterstain method. Scale Bar= 200 µm.*

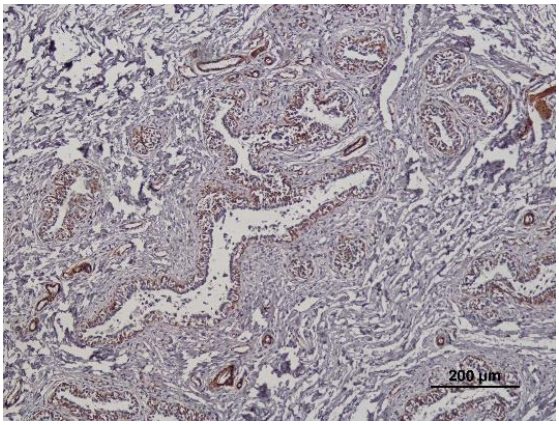


*Figure 36 - New-born donkey MG: TEBs. α-SMA immunostaining: MECs and blood vessels positive. Haematoxylin counterstain. Scale Bar= 200 µm.*

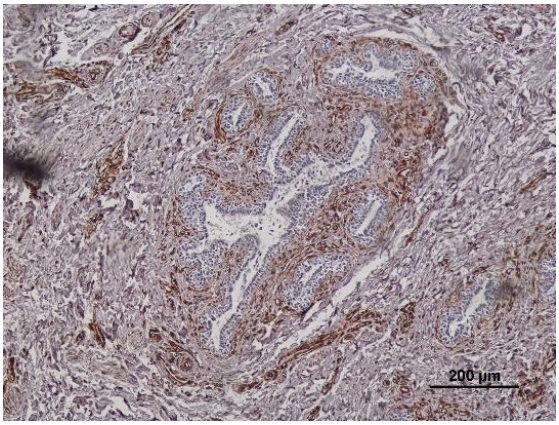


*Figure 37 - New-born donkey MG: TEBs. Vimentin immunostaining. IAS show a high marker expression. Haematoxylin counterstain. Scale Bar= 200 µm.*

In adult animals' samples, CK AE1AE3 highlighted the mammary epithelium, at the cytoplasm and cytoplasmic membrane, but its expression was heterogeneous. In lactating MG samples, the intensity of cytoplasmatic staining was usually reduced, with the lipid droplet contours highlighted (Fig. 38 and 39) whereas in non-lactational MG samples, the LEC were intensely stained (Fig. 40), allowing the observation of MEC hypertrophy in some samples (Fig 41).

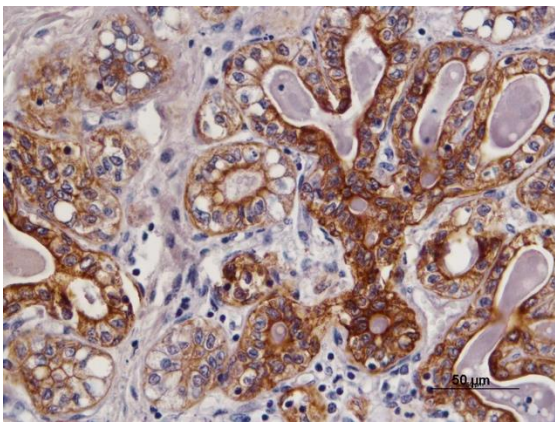


*Figure 38 - Donkey lactating MG. CK AE1AE3 immunostaining: heterogeneous staining in LEC layer, with some vacuolated LEC characterized by low-intensity cytoplasm staining. Haematoxylin counterstain. Scale Bar= 50 µm.*

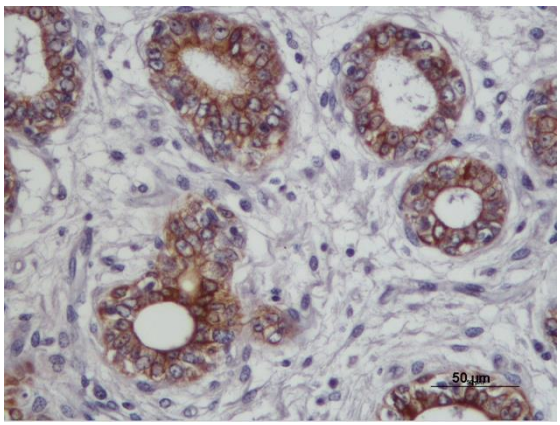


*Figure 39 - Donkey lactating MG. CK AE1AE3 immunostaining: LEC with low-intensity staining that delimitates the lipid droplets. Haematoxylin counterstain. Scale Bar= 50 µm.*

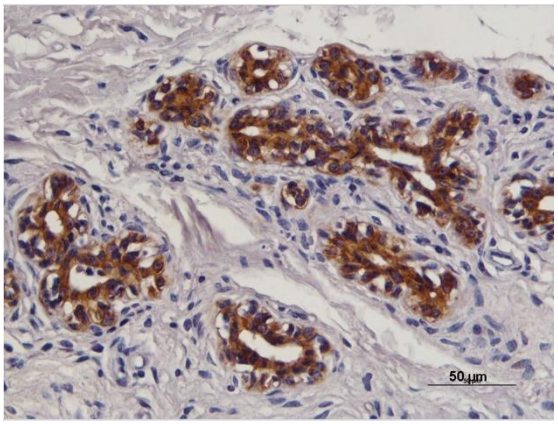


*Figure 40 - Donkey non-lactating MG. CK AE1AE3 immunostaining: LEC layer cytoplasm highly stained. Haematoxylin counterstain. Scale Bar= 50 µm.*

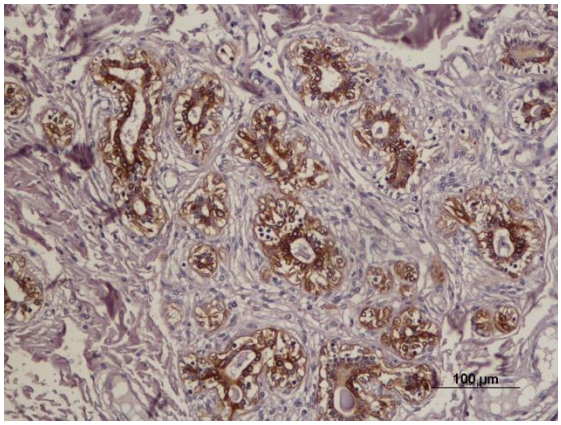


*Figure 41 - Donkey non-lactating MG. CK AE1AE3 immunostaining: LEC layer cytoplasm highly stained, and moderately stained MEC. Haematoxylin counterstain. Scale Bar= 100 µm.*

MECs showed expression of α-SMA**,** calponin (both at cytoplasm), and p63 (at the nucleus). Cytoplasmic markers highlighted the morphology of MEC, varying from fusiform to a stellate/vacuolated morphology. α-SMA expression was more intense in the non-lactating MG; during lactation, MEC usually showed a fusiform morphology, associated with a weaker expression (Fig. 42 and 43).

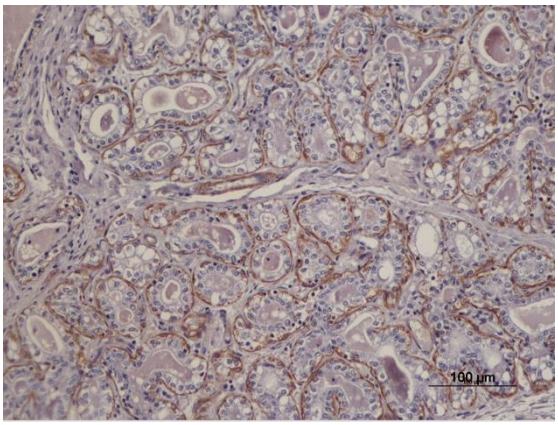


*Figure 42 - Donkey lactating MG. α-SMA immunostaining: note the fusiform morphology of the MEC layer, with a moderate staining intensity. Haematoxylin counterstain. Scale Bar= 100 µm.*

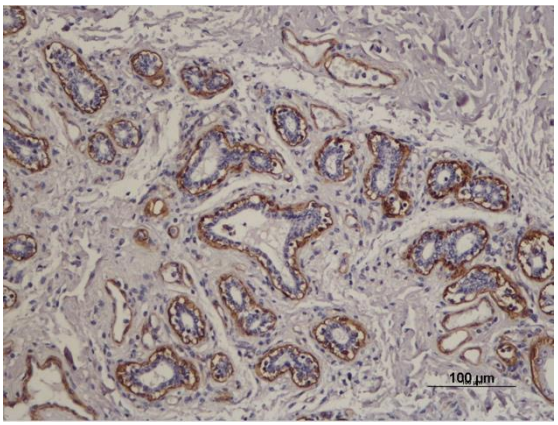


*Figure 43 - Donkey non-lactating MG. α-SMA immunostaining. Note the stellate morphology of the alveolar MEC, highlighted by the presence of a "clear space" between the LEC and the basement membrane. Haematoxylin counterstain. Scale Bar= 100 µm.*

P63 was expressed by the nucleus of basal/myoepithelial cells (Fig. 44). MEC nuclei assumed a wide variety of shapes, from the most spherical to the most elongated. This marker allowed the observation of the eccentric nuclear position in hypertrophied MEC (Fig. 45).

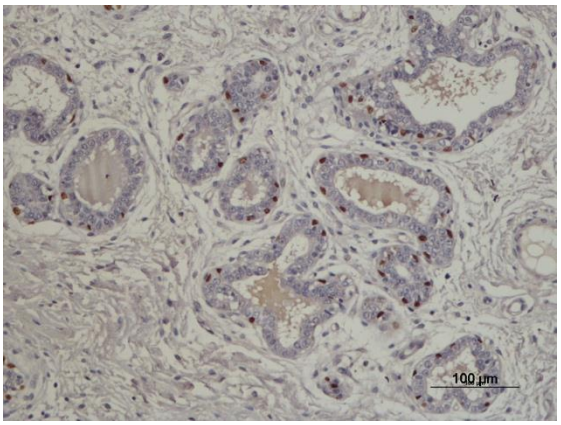


*Figure 44 - Donkey Lactating MG. p63 immunostaining in MEC. Haematoxylin counterstain. Scale Bar= 100 µm.*

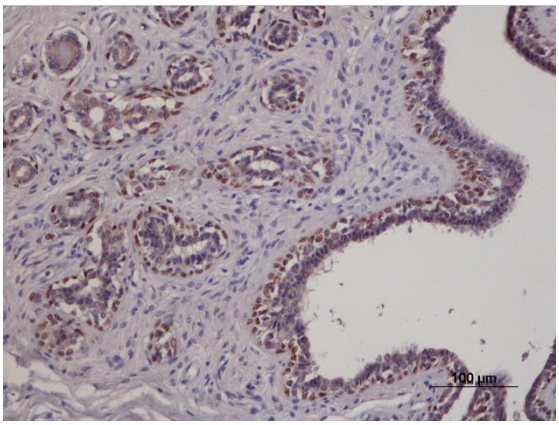


*Figure 45 - Donkey non-lactating MG. p63 immunostaining. Vacuolated MEC with eccentric nuclei. Haematoxylin counterstain. Scale Bar=100 µm.*

### 3.3 Stroma

The IAS showed a high vimentin expression, allowing a clear delimitation of the lobules (Fig. 46 and 47). Although not so evident, scattered stromal components in the IES also expressed α-SMA and calponin, suggesting the presence of small vessels. Moreover, the IAS of non-lactating MGs (Fig.47) showed more intense staining for vimentin than the IAS of lactating MGs.

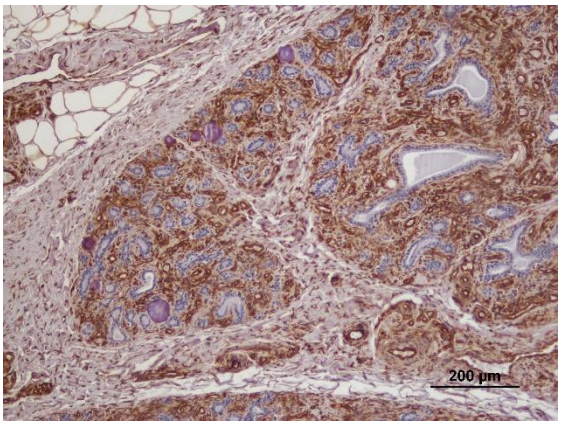


*Figure 46 - Donkey MG with lobular hyperplasia. Vimentin immunostaining: stained IAS delimitating lobular contours. Haematoxylin counterstain. Scale Bar= 200 µm.*

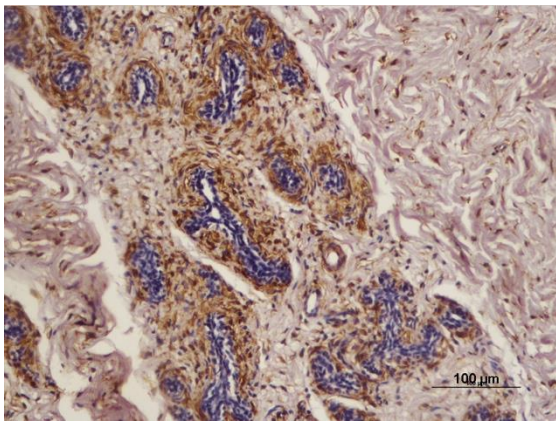


*Figure 47 - Donkey non-lactating MG. Vimentin immunostaining: IAS of small lobules with a high expression. Haematoxylin counterstain. Scale Bar=100 µm.*

Small **blood vessels** were evidenced in the stroma through the staining of its muscular *tunica media* by α-SMA and calponin and the staining of its *tunica intima* (endothelial cells) by vimentin (Fig.48). Furthermore, the arteries were easily distinguished from the veins through the expression of calponin (Fig. 49) and α-SMA (Fig. 50 and 51) since they have a more prominent tunica media than veins. These markers also help to differentiate between small blood vessels and ductules (smaller diameter ducts closer to the alveoli). The lactational mammary

gland exhibited a significant increase in the number of stained blood vessels and capillaries.

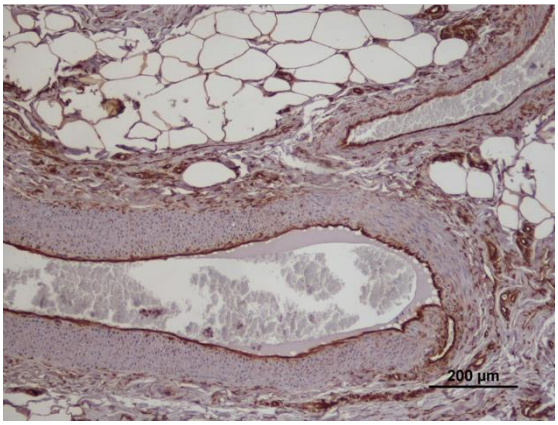


*Figure 48 - Donkey MG. Vimentin immunostaining. The thin endothelial layer of the blood vessels highly expresses vimentin. Haematoxylin counterstain. Scale Bar= 200 µm.*

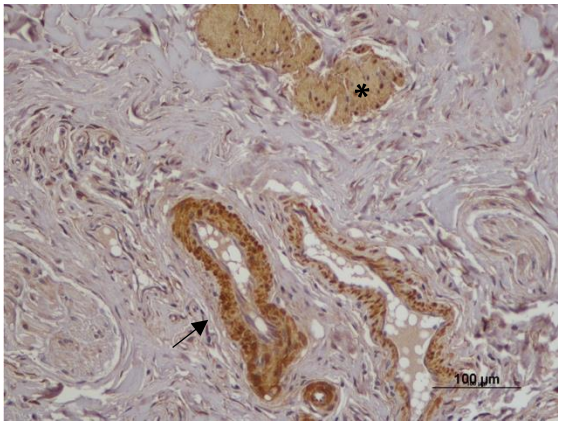


*Figure 49 - Donkey MG. Calponin immunostaining. Tunica media of the artery expressed calponin (arrow), and a small vein was also evidenced (arrowhead). SMF stained for calponin (*). Haematoxylin counterstain. Scale Bar= 100 µm.*

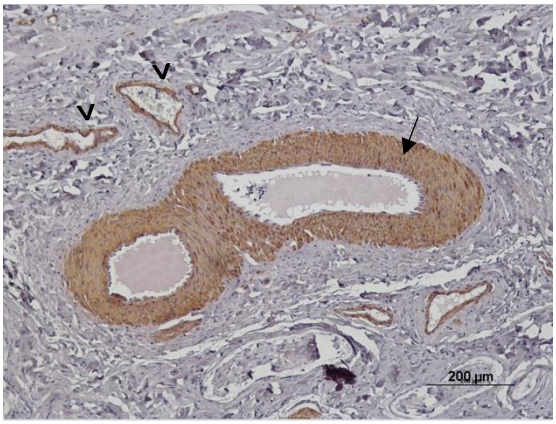


*Figure 50 - Donkey MG. α-SMA immunostaining. The tunica media of the artery (arrow) and small veins (arrowheads) were highlighted. Haematoxylin counterstain. Scale Bar= 200 µm.*

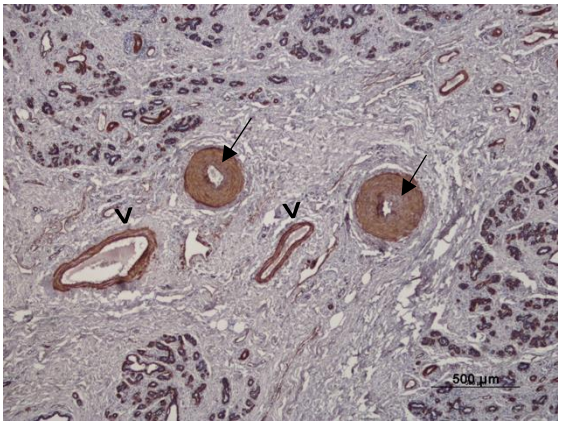


*Figure 51 - Donkey MG. α-SMA immunostaining. The tunica media of the arteries (arrows) and veins (arrowheads) were highlighted. Haematoxylin counterstain. Scale Bar= 500 µm.*

The following table has been formulated to concisely present the principal inferences and conclusions.

*Table 6 - Comprehensive and detailed summary of the main conclusions drawn from analysing different histological appearances of jennet's mammary gland.*

| | **Lactating Gland** | **Non-lactating Gland** | **Newborn** |
|---|---|---|---|
| **H&E** | **Hyperplastic** lobules; Presence or not of cytoplasmatic **lipid vacuolation**; variable amounts of **luminal secretion**; **LEC regularly cuboidal** in some samples. | **Small lobules** and alveoli, surrounded by a **prominent** mature interlobular and intralobular fibrous **connective tissue.** | **Limited** ductal **branching**; primary ductal structures in small aggregates (**TEBs**). |
| **CK AE1AE3** | **Reduced and heterogenous** staining intensity due to the presence of **lipid droplets** in LEC cytoplasm. | LEC **intensely** stained; **Contours** of the hypertrophied MEC evidenced. | Stained TEBs' **epithelial component**. |
| **Calponin** and **α-SMA** | **Low intensity** of marker expression; **Fusiform** MEC morphology. | **Intense** expression of α-SMA; Stellate and **hypertrophied** MEC morphology. | Stained **cap cells** of TEBs and blood vessels. |
| **p63** | **Few** noticeable MEC nuclei. | **Numerous** MEC nuclei were clearly marked. | Stained TEBs' **epithelial component**. |
| **Stroma** | Increase in number of stained **blood vessels** and capillaries by vimentin, calponin and α-SMA. | A significant region of the **IAS** was identified using vimentin labelling. | Vimentin showed that the **IAS** is less prominent than the IES. |

# 4. Histopathological alterations of donkey mammary gland

## 4.1 Metaplastic/proliferative mammary lesions

MGs from 10 adult jennies (15.4%) presented the following metaplastic/proliferative alterations: papillomatosis, characterized by intraductal epithelial papillary projections associated with duct ectasia (n=2; 3.1%) (Fig. 52); cystic apocrine metaplasia, characterized by cystically dilated ducts lined by benign apocrine epithelium (n=1; 1.5%) (Fig. 53), sebaceous or apocrine metaplasia (n=6; 9.2% and n=3; 4.6%, respectively), with multiple metaplastic alterations found in two animals (Fig. 54 e 55). Ductal squamous metaplasia has also been identified in ductal epithelium, in one sample (1.5%) (Fig. 54).

Apocrine metaplasia is characterized by epithelial cells with apocrine differentiation: enlarged cells, displaying a cuboidal, columnar, or polygonal morphology (Fig. 54). Sebaceous metaplasia was characterized by sebaceous epithelial cell differentiation (with clear cytoplasmatic vacuoles and a small eccentrically located nucleus (Fig 55). Squamous metaplasia was characterized by multiple layers of flattened squamous epithelium and loss of the bilayer epithelial conformation (Fig. 54).

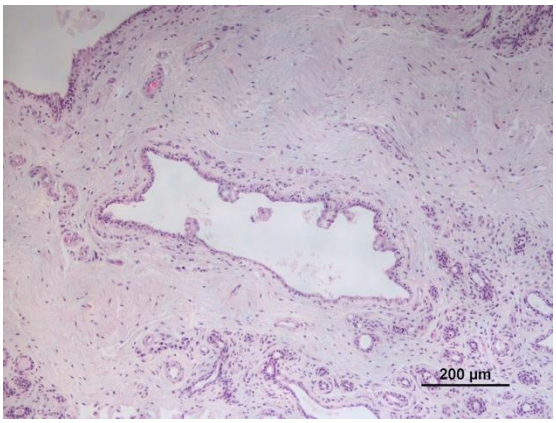


*Figure 52 - Donkey MG. Multiple intraductal epithelial papillary projections, associated with duct ectasia. H&E stain. Scale Bar= 200 µm.*

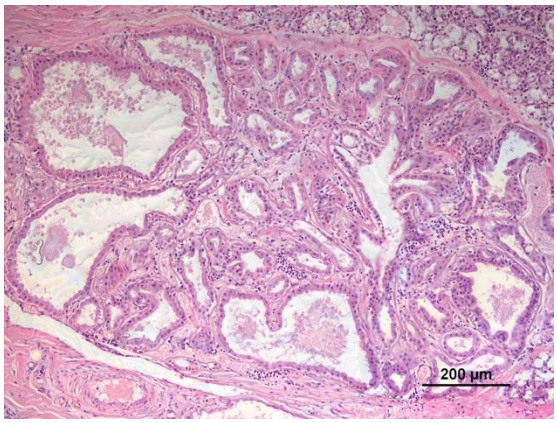


*Figure 53 - Donkey MG. Cystic apocrine metaplasia, characterized by cystically dilated ducts lined by benign apocrine epithelium. H&E stain. Scale Bar= 200 µm.*

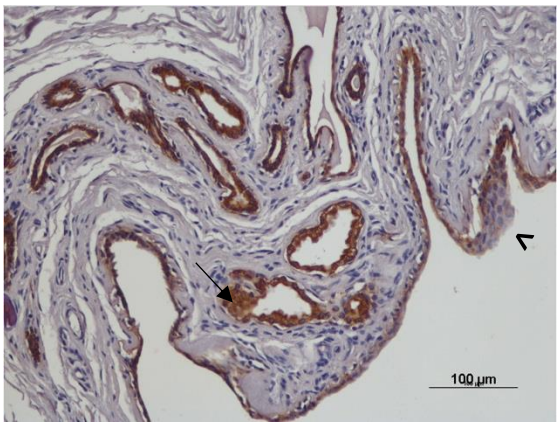


*Figure 54 - Donkey MG. CK AE1AE3 immunostaining. Mammary parenchyma with apocrine differentiation (arrow). Ductal epithelium with squamous metaplasia positive for CK (arrowhead). Haematoxylin counterstain. Scale Bar= 100 µm.*

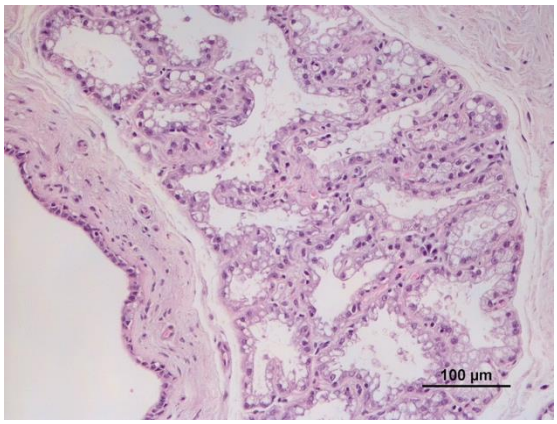


*Figure 55 - Donkey MG. Sebaceous metaplasia. H&E stain. Scale Bar = 100 µm.*

## 4.2 Psammoma bodies (PBs)

Mineralized concretions (psammoma bodies) were frequently observed (n=30;46.1%). Characterized by a body with concentric lamellated striations and a basophilic core (Fig. 56), they were usually found in fully differentiated secretory parenchymal areas. Considering the number of PBs observed, fifteen (23%) samples presented a small to moderate number of PBs while another fifteen (23%) showed numerous PBs. Interestingly, none of the prepubertal samples present PBs, and they were also uncommon in involuting MG. Mammary parenchymal areas were the common location of these mineralized concretions (Fig. 56 and 57).

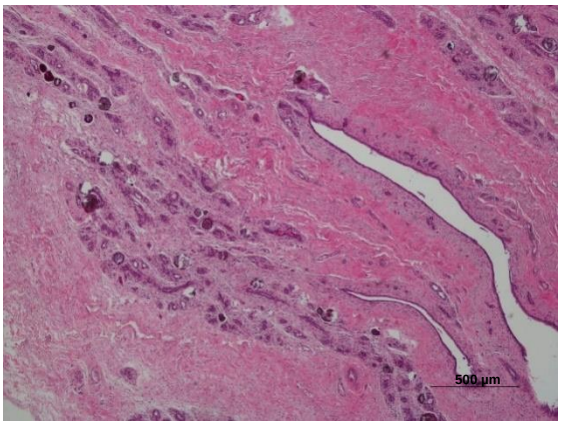


*Figure 56 - Donkey MG. Psammoma bodies with a basophilic core and concentric striations. H&E stain. Scale Bar= 500 µm.*

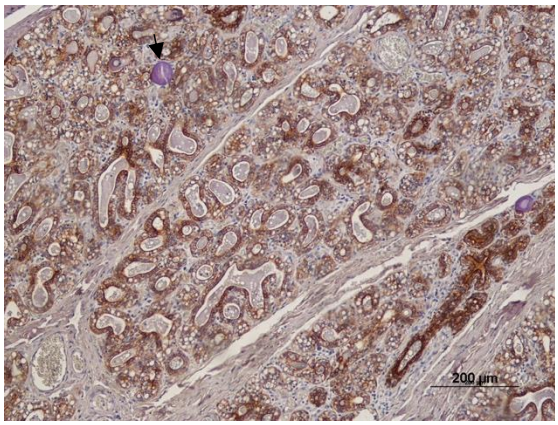


*Figure 57 - Donkey lactating MG. CK AE1AE3 immunostaining. Note the presence of a psammoma body communicating with alveolar lumen (arrow) inside the alveoli. Haematoxylin counterstain. Scale Bar= 200 µm.*

### 4.3 Mammary gland inflammatory infiltrate

In this study, foci of mononuclear inflammatory cells (lymphocytes and plasma cells) were identified in 18.5% of the samples (n=12/65), located essentially in the IAS (Fig. 58), highlighted by vimentin staining (Fig 59).


*Figure 58 - Donkey MG. Mononuclear inflammatory infiltrate (encircled). H&E stain. Scale Bar= 100 µm.*

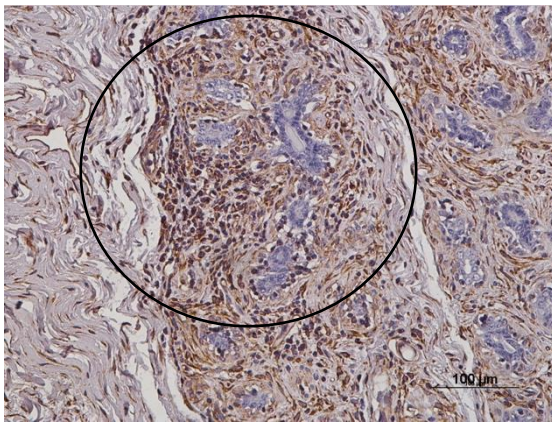


*Figure 59 - Donkey MG. Vimentin Immunostaining. Inflammatory cells in mammary parenchyma stain positively for vimentin. Haematoxylin counterstain. Scale Bar= 100 µm.*

In addition, four samples (n=4/65; 6.2%) were characterized by the presence of eosinophils in parenchymal areas. One of these samples, besides the periductal location of eosinophils, also showed mononuclear cells infiltrates at this location (Fig.60) and infiltration of eosinophils in udder's adjacent dermis (Fig. 61).

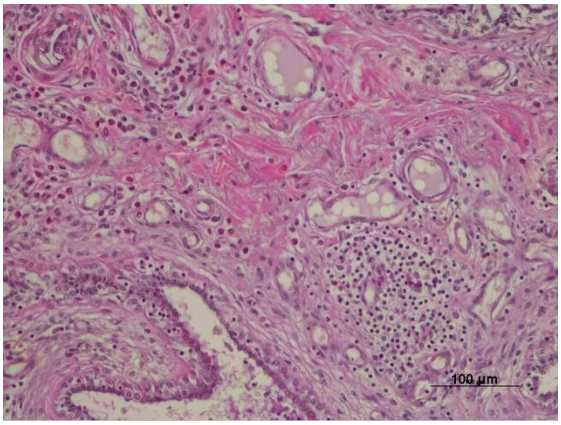


*Figure 60 -Donkey MG. Mixed inflammatory infiltrate of eosinophils and mononuclear cells in the periductal area. H&E stain. H&E, Scale bar= 100 µm.*

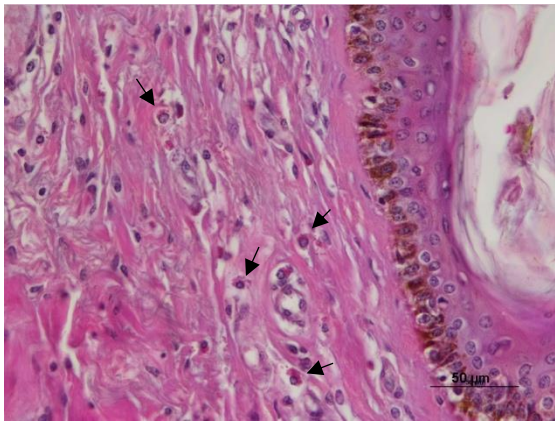


*Figure 61 – Donkey teat skin. Marked infiltration of eosinophils in the skin dermis (arrows). H&E stain. Scale bar= 50 µm.*

## 4.4 Other alterations

MEC hypertrophy was observed in twelve (18,5%) samples (Fig. 62-65). One of these samples also showed MEC hyperplasia in ducts and alveoli (Fig. 64 and 65).

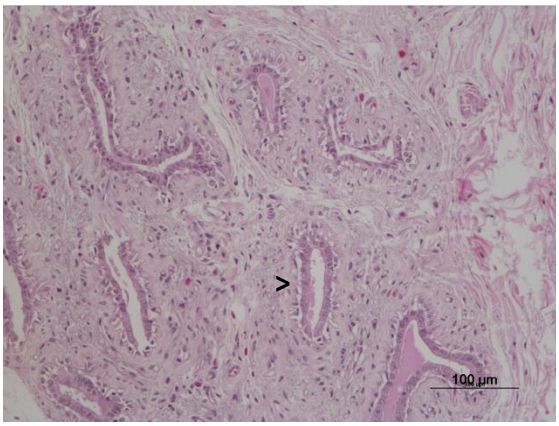


*Figure 62 - Donkey non-lactating MG. Alveolar–ductal MEC layer showing a prominent, clear, vacuolated cytoplasm (arrowheads). H&E stain. Scale bar = 100 µm.*

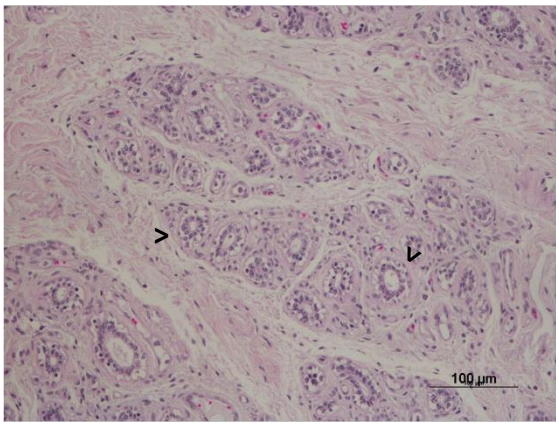


*Figure 63 - Donkey non-lactating MG. Alveolar–ductal MEC layer showing a prominent, clear, vacuolated cytoplasm (arrowheads). H&E stain. Scale bar = 100 µm.*

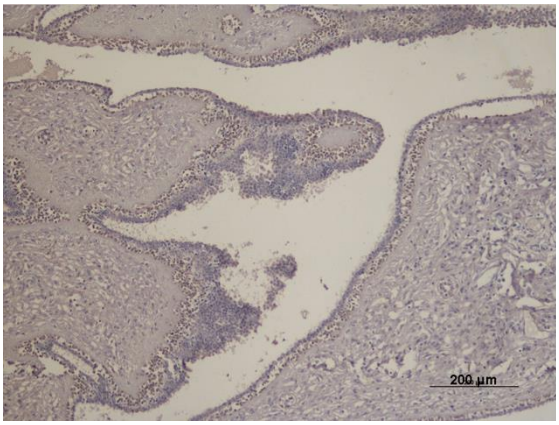


*Figure 64 - Donkey MG. p63 immunostaining. Hyperplasia and hypertrophy of ductal MEC layer. p63 evidences the numerous MEC cell nuclei. Haematoxylin counterstain. Scale bar= 200 µm.*

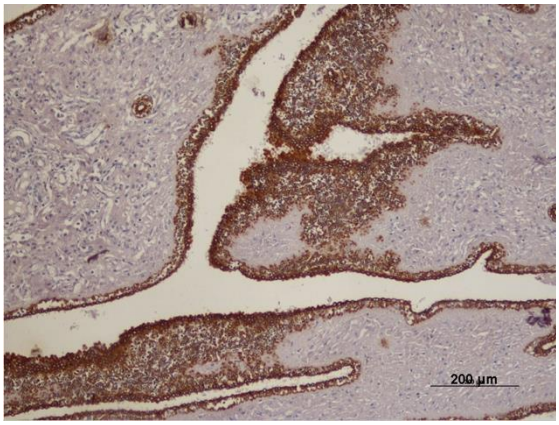


*Figure 65 - Donkey MG. CK AE1AE3 immunostaining. Hyperplasia and hypertrophy of ductal MEC layer. CK AE1AE3 stains the MEC cells contour. Haematoxylin counterstain. Scale bar= 200 µm.*

## V - Discussion

A comprehensive characterization of the donkey mammary gland histology can support the investigation of pathological processes affecting this organ, such as mastitis and proliferative lesions. Given that scarce information is available on this topic, the present study evaluated the histomorphological characteristics of the asinine MG.

### 1. Macroscopic and microscopic features of jennet mammary gland

Our results related to the external appearance of jennet's udder agree with the results by Kaskous and Pfaffl (2022), which classified the udder as bowl and globular and the teats shape as conical and cylindrical. Regarding the teat epidermis, we noted a darker appearance of the udder and teats supported by the increase of melanocytes in the basal layer of the epidermis. Sorenmo K. (2010) mentioned the same finding in dogs' mammary gland, which is associated with an increased number of melanocytes in this region.

The teat and udder epidermis showed minimal hair follicles and large adnexal glands differing in the teat orifice region, in which the hair and glands were inexistent. Also, dogs (Zappulli et al., 2019), cows (Nickerson & Akers, 2011), and dromedaries (Kausar et al., 2001; Cardiff et al., 2018), showed hairless teats and less hair in the udder. Koyama et al. (2003), who guided a study in mice, humans, and cows, referred that the key distinguishing feature of the teat epidermis was the presence of epidermal ridges. Our study also showed an increase of epidermal ridges in teats tip epidermis.

Donkey MGs evidenced a structural organization comparable to horses, with two paired mammary complexes (Chavatte-Palmer, 2002; Canisso et al. 2020; Hughes, 2020a; Hughes 2020b) exhibiting distinct histological morphologies according to the reproductive phase: prepubertal (inactive), fully developed lactating, and involuting MG.

Donkey's neonatal MG shows very little ductal branching and small bulbous epithelial structures consisting of tightly packed multiple-layered cells

with large nuclei and indistinct cell borders, which represent terminal-end-buds (TEBs).

Regarding the shape, size, and number of the lobular structures, it was found that in lactation the lobules are large, with numerous alveoli. A similar pattern of results was observed in mice (Masso-Welch et al., 2000; Yallowitz et al., 2014), and humans (Cardiff et al., 2018; Hughes, 2020a). Our results showed that most of the lactating lobules had luminal eosinophilic secretion. These findings are in accordance with findings reported by Sorenmo (2010) regarding the canine mammary gland.

After lactation, in humans, MGs go through an involution period of structural remodelling (Yallowitz et al., 2014). In this study, we observed that resting MG had smaller lobules due to the reduction of alveolar structures per lobule. Hassiotou & Geddes (2012) and Hughes (2020a) suggested the loss of the epithelium, in human and equines respectively, to be mediated by phagocytosis by the luminal epithelium, contrasting the old theory of recruiting macrophages from blood vessels and lymphatics to phagocyte epithelial components (Masso-Welch et al., 2000).

## 2. Immunohistochemical characterization of jennet mammary gland

This is the first study on the characterization of donkey's mammary gland using the immunohistochemistry technique. Previous studies in donkeys were based on the gross anatomy of the mammary gland, by direct observation and ultrasonographic methods, focusing on the improvement of milking systems and, consequently, the microbiological quality of milk (D'Alessandro et al., 2015; Hassan et al., 2016; Kaskous & Pfaffl 2022). Furthermore, this study also demonstrated the cross-reactivity of the biomarkers in donkey mammary tissues, by using antibodies developed to humans.

The study of Hughes (2020a), describing the histology of the teat and udder of the mare's mammary gland, the closest phylogenetically species to donkeys, using H&E routine methods, served as a comparative basis for the work reported herein. In addition, for discussing antibodies cross-reactivity in donkeys' tissues, given the lack of immunohistochemical studies in equids, were also

considered from the studies carried out in dromedaries (Kausar et al. 2001), mice (Masso-Welch et al., 2000; Davis & Fenton, 2013; LÍŠKA et al, 2016), humans (Hassiotou & Geddes, 2012; Cardiff et al.,2018), dogs (Sorenmo, 2010; Zappulli et al. 2019) and ruminants (Nickerson & Akers, 2011), the most studied animal species on this matter.

### 2.1 Teat

The basal layer of the teat epidermis and teat canal, the hair follicles (epithelial sheath and hair bulb), and the contouring cells of the sebaceous gland are stained positively for p63. The p63 protein has a crucial role in the hair follicle and skin appendages morphogenesis and is generally restricted to cells with high proliferative potential, being absent from cells that are undergoing terminal differentiation (Parsa et al., 1999; Mikkola , 2007; Shimomura et al., 2008). As a result, p63 expression is considered a marker of keratinocyte basal/progenitor cells of the epidermis and epidermal appendages (Tsujita-Kyutoku et al., 2003; Kai-Hong et al., 2007). Weber et al. (2019) described that in new hair follicles, with less than 24 hours, all the keratinocytes (internal and external) express p63. In hair follicles with more than a day, only the external basal layer is stained, corresponding to the more proliferative cells (Parsa et al., 1999; Weber et al., 2019). Considering the similar expression pattern in jennet's tissues, the role of p63 in donkey skin is probably comparable to other species. Expression of p63 has been detected in human and canine sebaceous glands by Reis-Filho et al. (2002) and Saraiva et al. (2008), respectively. Saraiva et al. (2008) mentioned that most mature sebocytes were negative for p63 but some, especially those nearest the basal cells, exhibited positivity, which is in accordance with the results of our study. Saraiva et al. (2008) and Obaidat et al. (2006) also mentioned positive p63 staining for MEC in the sweat glands.

Although with differences in staining intensity, most skin epithelial cells stained positively for CK AE1AE3, including the epithelial sheath of the hair follicle, the epidermal *stratum basale*, sweat glands, and the sebaceous gland (specially the basal layer). Haihong et al. (2006), who used CK AE1AE3 in rat skin samples, observed positivity in hair follicles and sebaceous glands. Furthermore, Raposio et al. (2007), also proved the same reactivity for CK

AE1AE3 in human skin hair follicles. Besides skin structures, CK AE1AE3 stained the mammary teat canal epithelium; entering the teat orifice; in the teat canal, CK AE1AE3 highlights its epithelium, that continues from the skin epidermis, being characterized by a thick stratified squamous epithelium until the entrance of the gland cistern. In gland cistern, the CK AE1AE3 specially stained the luminal layer, while p63, α-SMA and calponin stained the external basal layer. Also, in mice (Barbosa et al., 2019), cows (Alsodany & Al-Derawi, 2018), and goats (Pattison, 1952) the epithelium of the gland cistern assumes a bilayer conformation.

The arrector pili muscles, present in the jennet's teat skin, showed immunopositivity for α-SMA and calponin. The APM connects the bulge region of a hair follicle permanent portion of the dermis (Sato et al., 2012). These muscle fibres are beneficial for the hair follicle to cope with the movement of the hair shaft (Morioka, 2011).

Sweat glands are widely distributed in the jennet's teat skin and stained positive for CK AE1AE3 in LEC and for α-SMA, p63, calponin and vimentin in MEC. Studies in human skin showed that MEC layer of sweat glands express SMA, p63 and calponin (Obaidat et al., 2006), which agrees with our results. An interesting result of the present study were the positivity for vimentin in MEC, since vimentin is not specific for these cells. We also confirmed the muscular nature of these vimentin-positive cells using α-SMA and calponin. A similar pattern of results was obtained in Eckert et al. (1994) who mentioned that vimentin immunoreactivity was restricted to MEC and some cells of the coiled duct in normal sweat glands of human skin. However, these authors did not test for α-SMA to prove the real MEC nature of the reactive cells. In cow's skin, Gulbahar et al. (2002) also mentioned that spindle myoepithelial cells of sweat glands stain for α-SMA and vimentin.

In the teat, the presence of a circular SMS with longitudinal and transverse SMF was observed, being highlighted by α-SMA, vimentin, and calponin. SMS keep the teat canal tightly closed avoiding bacteria from progressing upwards, into the mammary parenchyma (Nickerson & Akers, 2011; Khan et al., 2020). Due to its fibromuscular nature, it participates also in milk ejection (Cardiff et al., 2018; Barbosa et al., 2019). The presence of a SMS had been also mentioned in equine (Hughes, 2020a), bovine (Nickerson & Akers, 2011; Khan et al, 2020),

canine (Sorenmo, 2010; Zappulli et al.,2019; Evans & Christensen, 2013), and human teats/nipples (Montagna, 1970; Koyama et al., 2013).

### 2.2 Mammary parenchyma

Mammary epithelium was consistently positive for CK AE1AE3, which has highlighted distinct morphologies of LEC. A more dispersed CK AE1AE3 staining was observed in active secretory cells compared to LEC in inactive glands, a consequence of the presence of cytoplasmic lipidic vesicles. Other studies in dogs (Davis & Fenton, 2013; Zappulli et al., 2019) and mice (Masso-Welch et al., 2000; Cardiff et al., 2018) describe similar LEC features during lactational activity.

In non-secretory MGs, CK AE1AE3 intensely stained the LEC layer, characterized by small sized packed cells. Sometimes, it was difficult to histologically differentiate the inactive alveoli from the intralobular ducts, due to their similar appearance. These common observations were also made by different authors who studied MG histology in horses (Hughes, 2020a), dogs (Sorenmo, 2010; Zappulli et al., 2019), humans (Cardiff et al.,2018), mice (Masso-Welch et al., 2000; Davis & Fenton, 2013), cows (Nickerson & Akers, 2011) and dromedaries (Kausar et al., 2001).

In H&E-stained tissues, the MEC can be hardly distinguished from the other cell types. To facilitate its identification, myoepithelial cell markers were used, including α-SMA, calponin and p63. The expression of α-SMA (Hirayama et al., 2003; Reesink et al., 2009; Bussche et al., 2017; Hughes 2020a) and calponin (Brocca et al., 2020) has previously been demonstrated in equine MG, whereas p63 were not. We verified that these markers can also be used in donkey MG to identify these cells, as it happens with dogs (Espinosa de los Monteros et al., 2002; Gama et al., 2003; Ramalho et al., 2006; Sorenmo, 2010; Toniti et al., 2010; Rasotto et al., 2014; Zappulli et al., 2019; Łopuszyński et al., 2019), mice (Deugnier et al., 1995; Masso-Welch et al., 2000; Yallowitz et al., 2014), cows (Hellmén & Isaksson, 1997; Alkafafy et al., 2012; Marettová & Maretta, 2018) and humans (Gugliotta et al., 1988; Dusek et al., 2012).

Expression of p63 by MEC nuclei in JMGs was higher in non-lactating glands than in lactating glands. Since marker p63 is crucial for sustaining the

mammary epithelial stem cells' proliferative potential and self-renewing capacity (Ramalho et al., 2006; Gatti et al., 2019), we defend that the proliferative activity of MEC in JMGs is higher in non-lactating periods and practically insignificant during lactation. These findings are consistent with previous research made in mice that also proved a slowdown of cell proliferation during lactation (Yallowitz et al., 2014; Cardiff et al., 2018).

In lactational MG, a more fusiform morphology in alveolar MEC was observed, due to the stretching resultant from luminal high pressure caused by the presence of milk. Masso-Welch et al. (2000) and Sorenmo (2010) also mentioned the thinning of MEC during the MG active secretory period, in mice and dogs, respectively. In non-lactating MG states, we observed different morphologies of alveolar MEC. α-SMA and calponin are cytoplasmic myoepithelial markers, and better illustrate the stellate, clear, and vacuolated MEC cytoplasm. In canine MG, different MEC morphologies have been described: it is hypothesized that resting MEC have an elongated shape and flattened nuclei, while in a proliferative state, cells are called "hypertrophic" and are easily identified by their polygonal shape with vacuolated cytoplasm and ovoid nucleus (Espinosa de los Monteros et al., 2002; Zappulli et al., 2019; Łopuszyński et al., 2019).

### 2.3 Stroma

Using vimentin, smooth muscle fibres and mesenchymal elements (such as myofibroblasts, vessels, and inflammatory cells) were evidenced in donkey MG. We verified that IAS showed a higher intensity staining compared to IES, evidencing the more cellular and muscular nature of the stroma surrounding the alveolar structures. The findings are directly in line with previous research on mice, humans, and equines, which highlighted the presence of cellular elements such as fibroblasts, microvasculature, inflammatory cells, and muscle filaments in IAS (Cardiff et al., 2018; Hughes, 2020a). Moreover, vimentin allowed to better delimitate the lobules in size due to the staining contrast observed between the two-types of stroma. α-SMA and calponin also confirmed the presence of contractile components, irregularly scattered in the connective tissue between the alveoli or lobules and along the intralobular ducts. Marettová & Maretta (2018),

using anti-alpha SMA antibodies in bovine MG, obtained similar results regarding the stromal area. Comparably to dogs and human's mammary stroma (Zappulli et al., 2019; Cardiff et al.,2018), in jennets the MG stroma is arranged into a looser IAS and a denser and sparsely cellular IES.

The presence of blood vessels was evidenced by vimentin, α-SMA, and calponin in the interlobular area. Vimentin is the sole intermediate filament protein of endothelial cells lining the inner surface of large blood vessels. Vimentin might help endothelial cells to withstand the mechanical forces exerted by blood flow and blood pressure (Schnitzler et al., 1998). It is hypothesized that secreted vimentin could also mediate the movement of circulating blood cells across the endothelium, a process in which activated macrophages and activated platelets participate (Fidler & Brodey, 1967; Sorenmo, 2010). The blood vessels' muscular wall also labels for α-SMA and calponin (Brown et al., 2012), more specifically in the tunica media. In lactating JMGs, an evidenced augment of vascularization was observed. These findings are consistent with previous research: in dogs, Sorenmo (2010) described "numerous small, congested blood vessels" in active glands; Davis & Fenton (2013) mentioned an "intimate network of capillaries and lymphatics" in mice' active glands; and in human breast, Hassiotou & Geddes (2012) also described the "more visible" blood vessels due to supporting milk production.

In this study, we verified that resting JMGs have a much more abundant IES than lactating MGs. As described by Kausar et al. (2001) in dromedaries, at the end of the lactating period, the parenchyma is replaced by loose connective tissue, a possible explanation for the increase in IES volume. During lactation, the lobules expand due to milk secretion and the connective tissue stroma becomes more elastic to adjust and agglomerate the hypertrophic lobules (Nickerson & Akers, 2011; Biswas et al., 2022). A decrease in the surrounding IES in lactating states, due to the expansion of the epithelial parenchyma, was also mentioned in mice (Masso-Welch et al., 2000; LÍŠKA et al., 2016), humans (Hassiotou & Geddes, 2012; Cardiff et al.,2018) and dogs (Sorenmo, 2010; Davis & Fenton, 2013; Zappulli et al., 2019).

In non-lactating JMGs, vimentin showed a high IAS staining probably due to the more compacted intralobular connective tissue during this period. On the

contrary, lactating JMGs showed a sparse and scattered expression of vimentin in IAS, which suggests a greater spacing of the filaments.

Regarding the stromal component of neonatal MG, vimentin shows better staining, near the TEBs, which determines the limit of the future lobe. Studies in mice showed that vimentin expression is supportive of the basal/progenitor mammary epithelial cell population in mammary gland development (Peuhu et al., 2017). In short, the mammary gland of a new-born donkey shows a rudimentary denser “intralobular” connective tissue stroma surrounding the rudimentary epithelial structures. CK AE1AE3 stained both body cells and cap cells of TEBs showing its epithelial nature at this stage. A more specific marking for cap cells was achieved by α-SMA and calponin which emphasized the stellated and vacuolated appearance of these cells. As previously theorized, the vacuolated morphology of the MEC is suggestive of the intense activity of these cells. Also, Spaas et al. (2012) in equines and Biswas et al. (2022) in humans mentioned, that in developmental stages, the external layer of cap cells of TEBs, which will give rise to the MEC layer, is identified by α-SMA marker and calponin. Biswas et al. (2022) used keratin 5 and 14 (keratins specific of basal/MEC) to stain cap cells, proving that TEBs’ external layer expresses several markers for basal lineage, supporting our results. Furthermore, p63 showed a strong expression on TEB’s epithelial component. It is theorized that p63 is essential for proper mammary gland development and that cell adhesion is fundamental for ensuring the proper architecture and function of the mammary epithelium (Dusek et al., 2012). We can speculate that the strong expression of p63 in TEBs probably reflects its importance as a maintenance/proliferation factor of the basal epithelial compartment, where mammary stem/progenitor cells are known to reside (Yallowitz et al., 2014).

### 3. Histopathological alterations of donkey mammary gland

Although no macroscopic proliferative lesions were observed, some MG samples showed histological proliferative/metaplastic alterations, such as papillomatosis, apocrine, sebaceous, and squamous metaplasia. Both areas of apocrine and sebaceous metaplasia were frequently visualized in alveoli and ducts; the squamous metaplasia was observed in the ductal epithelium.

Ductal papillomatosis, characterized by intraductal epithelial papillary projections, have been described in several species such as humans and dogs (Zappulli et al., 2019; Kulka et al., 2021; Li & Kirk, 2022).

In humans, the apocrine change is the most common metaplastic alteration in benign mammary tissue, being extremely frequent as an accompanying factor of ductal hyperplasia (up to 87% of the cases) (Rath-Wolfson et al., 2010). Studies in humans (Celis et al, 2007), non-humans' primates (Cline, 2006) and mice (Okamoto et al., 2010) have shown that it can be considered a premalignant lesion. Celis et al. (2007) stated that invasive apocrine carcinomas evolve from apocrine metaplasia of normal breast epithelia.

As MGs are modified apocrine glands, sebaceous metaplasia can be derived from mammary pluripotent stem cells (basal cells) (Chang et al., 2007; Grandi et al, 2011), which justifies its frequent location onto the alveolar and ductal epithelium. Sebaceous metaplasia has also been identified in humans (Chang et al., 2007; Grandi et al., 2011; Kurilj et al., 2012) and dogs (Chang et al., 2007).

Regarding squamous metaplasia, it was detected in only one sample, in the ductal epithelium where the bilayer conformation (LEC and MEC) was unrecognized. In humans, squamous metaplasia arising in nonneoplastic breast parenchyma is rarely reported, and its exact origin in the breast is not clear (Reddick et al., 1985; Hurt et al., 1988; Rath-Wolfson et al., 2010). The mammary glandular epithelium is normally non-keratinized; however, some authors support the hypothesis of myoepithelial origin of the squamous metaplasia in human breast (Reddick et al., 1985; Rath-Wolfson et al., 2010). In horses, mammary adenomas can show squamous metaplasia with a marked increase in the number of epithelial layers showing classic stratified epithelium features (Spadari et al., 2008). In dogs, mammary squamous cell carcinomas arising from squamous differentiation of mammary epithelium are more invasive and aggressive than squamous cell carcinoma arising from local cutaneous tissue (Sharkey et al, 2020).

Future studies in jennet mammary glands should be carried out to study the presence of proliferative alterations, which were rarely observed in our samples.

Psammoma bodies (PBs) were a very frequent finding. Nonetheless, in the current study, samples of weakly developed mammary glands, corresponding to new-born or young animals, did not show any PBs. Since PBs may result of entrapping the waste products of a previous lactation (Riba Marta et al., 2021), it is expectable that virgin animals fail to present these concretions. Several authors pointed that, in most species, these structures can be observed in MG tissue or milk throughout lactation, except in virgin animals or in the colostrum of primiparous animals, showing an association with ageing (Nickerson & Sordillo, 1985; Sordillo & Nickerson, 1986; Claudon et al., 1998; Riba Marta et al., 2021).

Regarding the most frequent location of these bodies, it appears they have a tropism to the fully differentiated secretory parenchymal areas. A possible explanation for its regular location is based on its origin: waste products accumulate within the alveolar LEC and the alveolar lumen and are subsequently translocated into the interstitial spaces (McFadyean, 1930; Riba Marta et al., 2021). Our results are in line with previous publications on PBs location (McFadyean, 1930; Nickerson et al., 1985; Sordillo & Nickerson, 1986; Claudon et al., 1998; Eighmy et al., 2018).

A mononuclear inflammatory infiltrate is common finding within MG tissue. A healthy MG contains myeloid and lymphoid cells, mainly located within the lobules rather than in mammary fat or mammary stroma (Goulabchand et al., 2020). These infiltrates may be present in neoplastic or non-neoplastic MGs (Carvalho et al., 2011). The presence of mononuclear inflammatory cells was a common finding in JMGs. We investigated whether there was any association between its presence and an advanced age, but the lack of data on the age from many samples did not allow to withdraw any conclusions.

Vimentin was a useful marker in the identification of these cells. As vimentin is a mediator of cell movement across the endothelium of blood vessels, activated macrophages, apoptotic T lymphocytes, aged neutrophils, and platelets, express this marker (Chu et al., 2000; Sorenmo, 2010; Mor-Vaknin et al., 2013; Battaglia et al., 2018).

Previous studies had proven that MG mononuclear inflammatory infiltrates may be associated with the progression of mammary neoplasia in dogs (Carvalho

et al., 2011; Giambrone et al., 2022), cats (Hayes & Mooney, 1985) and mice (Russo & Russo, 2000); it is also a common feature of chronic mastitis in horses (Conte & Panebianco, 2019; Podico et al., 2021), cows (Chandler, 1970; Hillerton & Berry, 2005; Conte & Panebianco, 2019; Bianchi et al., 2019), sheep (Maestrale et al., 2013), dogs (Murai et al., 2013) and humans (Garcia-Rodiguez & Pattullo, 2013; Eyselbergs et al., 2017; Freeman et al., 2017).

The existence of eosinophilic infiltration in JMGs was rarely observed; it was identified in the mammary parenchyma of three samples (3/42; 7.1%). Interestingly, in one of these samples, eosinophils were also observed in the adjacent skin dermis. In most species, the presence of eosinophils in the mammary tissue is considered a rare finding.

As described in humans, eosinophil infiltration may be found in case of eosinophilic mastitis (Bajad et al., 2019), which in donkeys (Maia et al., 2016) and mares (Souto et al., 2019; Tartor et al., 2020) can be observed in Pythiosis, caused by *Pythium insidiosum* infection. Equidae skin contacts with contaminated water and motile zoospores penetrated the dermis through hair follicles, causing folliculitis and furunculosis and subsequent spreading of infection to the glandular parenchyma (Maia et al., 2016; Souto et al., 2019; Tartor et al., 2020). One of our samples showed eosinophils spread in the skin and mammary parenchyma which might be suggestive of Pythiosis. However, the diagnosis was not confirmed, as we did not find concordant clinical evidence.

## VI - Conclusion

The following study has investigated donkey's MG, and the results have provided valuable insights. The macroscopic and histological features of the donkey MG were found to be similar to those of the equine MG, including the teat and mammary parenchyma. The antibodies employed in this study displayed cross-reactivity with donkey tissues, which indicates a similar staining pattern to humans and other animal species. This presents a promising prospect for utilizing these immunohistochemical cell markers in future studies. The CK AE1AE3 antibody was able to distinguish between varying epithelial cell types in the mammary gland. Furthermore, the expression of α-SMA and calponin by the myoepithelial cells of ducts and alveoli highlighted their distinct morphological features. The vimentin antibody was found to stain the stromal component, including the intra- and extralobular stroma. Lastly, the p63 antibody specifically stained the basal/myoepithelial cells of the mammary gland. These findings are of particular significance in advancing our knowledge of the MG, not only in donkeys but also in other animal species, including humans. The implications of this study are substantial and will undoubtedly contribute to the development of future research in this field.

It is vital to acknowledge the limitations of this study. Although we made significant strides in our research, we also faced several obstacles that hindered our ability to draw more conclusive results. For instance, the lack of samples from newborn animals and the absence of precise information on the animal's age, their previous reproductive history or the stage of the oestrous cycle, forced us to group the samples into broader categories, limiting the depth of our analysis. Additionally, due to the scarcity of research on donkey MG and limited research on the use of immunohistochemical markers in MGs of other animal species, we were unable to strengthen our conclusions. During the study, we encountered several samples with putrefied appearances, making it challenging to discern the tissue architecture and therefore compromising its use to gather information. Finally, the limited time and financial support, restricted the number of samples stained using the indirect immunohistochemistry technique. Despite these limitations, we believe that our findings provide valuable insights into the field of donkey mammary gland research.

The mammary gland of donkeys is an infrequent site for the occurrence of neoplastic lesions. However, a few proliferative/metaplastic alterations were observed, and their potential to represent preneoplastic conditions is yet to be determined. The scarcity of mammary neoplasia in donkeys makes it intriguing to understand the underlying reasons.

This study provides veterinary pathologists with valuable information on the physiology of the donkey mammary gland, aiding in their differential diagnosis of its developmental changes. The proposed method of characterizing the histological phases of the mammary gland based on its activity holds promise. Nevertheless, further research with a larger sample size is paramount to investigate the association between the phase of the oestrous cycle and the gland's histological appearance. Future investigations could incorporate macro and microscopic analysis of donkey ovaries to determine the reproductive cycle phase for comparative purposes. The measurement of progesterone (P4) levels in the blood is also a valid method for determining the animal's oestrous cycle phase. By conducting such studies, we can expect to unravel the mystery behind the rarity of mammary neoplasia in donkeys and ensure better care for their mammary gland health.

## VII - References


ABDALKHANI A. [et al.]. nipple connective tissue and its development: insights from the K14-Pthrp mouse. *Mechanisms of Development*. 115(1-2). (2002). 63–77.

ALKAFAFY M., RASHED R., & HELAL A. Immunohistochemical studies on the bovine lactating mammary gland (*Bos Taurus*). *Acta Histochemica*. 114(2). (2012). 87–93.

ALSODANY A. & AL-DERAWI K. Comparative histological study of teat in jenubi cow and her crossbreed. *Journal of Global Pharma Technology*. 10(11). (2018). 196-200

BAI L. & ROHRSCHNEIDER L. s-SHIP Promoter expression marks activated stem cells in developing mouse mammary tissue. *Genes & Development*. 24(17). (2010). 1882-1892.

BAJAD S. [et al.]. Eosinophilic mastitis: a chameleon disease in rheumatologists' domain. *Indian Journal of Rheumatology*. 14(3). (2019). 241-243.

BARBOSA A. Spontaneous mammary tumors in domestic rats (*Rattus Norvegicus*). Instituto de Ciências Biomédicas Abel Salazar, Universidade do Porto [s.n.], 2019. Relatório Final de Estágio: Mestrado Integrado em Medicina Veterinária.

BARBOSA F. [et al.]. Carcinoma mamário ductal invasivo em uma vaca. *Acta Scientiae Veterinariae*. 46(1). (2018). 288.

BATTAGLIA R. [et al.] Vimentin on the move: new developments in cell migration. *F1000Research*. (2018). 1796.

BESSA A. [et al.]. Age-related linear and nonlinear modelling of semen quality parameters in miranda donkeys. *Italian Journal of Animal Science*. 20(1). (2021). 1029–1041.

BIANCHI, R. [et al.] Pathological and microbiological characterization of mastitis in dairy cows. *Tropical Animal Health And Production*. 51(7). (2019). 2057-2066.

BISWAS S. [et al.] The mammary gland: basic structure and molecular signaling during development. *International Journal Of Molecular Sciences*. 23(7). (2022). 3883.

BOYCE S. & GOODWIN S. Mammary gland neoplasia in a canadian mare: challenges of diagnosis and treatment in a rural setting. *The Canadian Veterinary Journal*. 58(6). (2017). 628-630

BROCCA G. [et al.] Case report of a mare diagnosed with a metastatic mammary carcinoma after the excision of a recurrent intraocular neuroepithelial tumor. *Animals*. 10(12). (2020). 2409.

BROWN P. [et al.] Fibroepithelial polyps of the vagina in bitches: a histological and immunohistochemical study. *Journal of Comparative Pathology*. 147(2-3). (2012). 181-185.

BUSSCHE L. [et al.] Carcinoma of the mammary gland in a mare. *Equine Veterinary Education*. (2017). 370–5.

BUSSOLATI G. [et al.] The immunohistochemical detection of lymph node metastases from infiltrating lobular carcinoma of the breast. *British Journal of Cancer*. 54(4). (1986). 631–636.

CANISSO I., PODICO G., ELLERBROCK R. Diagnosis and treatment of mastitis in mares. *Equine Veterinary Education*. (2020). 320-326.

CARDIFF R. [et al.]. *Mammary gland*. In: TREUTING P. [et al.] eds. Comparative Anatomy and Histology: A Mouse, Rat, and Human Atlas. Second Edition. London, UK: Elsevier, Academic Press, 2018. ISBN 978-0-12-802900-8. p. 487–509.

CARVALHO M. [et al.] T-Lymphocytic infiltrate in canine mammary tumours: clinic and prognostic implications. *In Vivo.* 25(6). (2011). 963-969.

CELIS J. [et al.] Characterization of breast precancerous lesions and myoepithelial hyperplasia in sclerosing adenosis with apocrine metaplasia. *Molecular Oncology*. 1(1). (2007). 97-119.

CHANDLER R. Experimental bacterial mastitis in the mouse. *Journal of Medical Microbiology*. 3(2). (1970). 273–282.

CHANG S-C. [et al.] Mammary carcinoma with sebaceous differentiation in a dog. *Veterinary Pathology*. 44(4). (2007). 525–527.

CHAVATTE-PALMER P. Lactation in the mare. *Equine Veterinary Education*. 14(S5). (2002). 88–93.

Chu P., Wu E., Weiss L. Cytokeratin 7 and cytokeratin 20 expression in epithelial neoplasms: a survey of 435 cases. *Modern Pathology*. 13. (2000). 962–972.

CLAUDON C. [et al.] Proteic composition of corpora amylacea in the bovine mammary gland. *Tissue and Cell.* 30(5). (1998). 589–595.

CLINE J. [et al.] Hormonal effects on the mammary gland of postmenopausal nonhuman primates. *Breast Disease*. (2006). 59–70.

COLAVITA, G. [et al.] Hygienic characteristics and microbiological hazard identification in horse and donkey raw milk. *Veterinaria Italiana*. 52(1). (2016). 21-9.

COLLI L. [et al.] Detecting population structure and recent demographic history in endangered livestock breeds: the case of the italian autochthonous donkeys. *Animal Genetics*. 44(1). (2012). 69–78.

CONTE F. & PANEBIANCO A. Potential hazards associated with raw donkey milk consumption: a review. *International Journal of Food Science*. (2019). 1–11.

CONTRI A. [et al.] Effect of the season on some aspects of the estrous cycle in martina franca donkey. *Theriogenology.* 81(5). (2014). 657–661.

COULOMBE P. & WONG P. Cytoplasmic intermediate filaments revealed as dynamic and multipurpose scaffolds. *Nature Cell Biology*. 6(8). (2004). 699-706.

D'ALESSANDRO A., MARIANO M., MARTEMUCCI G. Udder characteristics and effects of pulsation rate on milking machine efficiency in donkeys. *Journal of Dairy Research*. 82(1). (2015). 121–128.

DANIEL C. & SMITH G. The Mammary Gland: A Model or Development. *Journal of Mammary Gland Biology Neoplasia*. 4(1). (1999). 3-8.

DAVIS B. & FENTON S. *Mammary gland*. In: HASCHEK W. [et al.]. Haschek And Rousseaux's Handbook Of Toxicologic Pathology. Third Edition. Amsterdam: Elsevier, Academic Press, 2013. ISBN 978-0-12-415759-0. p. 2665-2694.

DE PALO P., AUCLAIR-RONZAUD J., MAGGIOLINO A. Mammary gland physiology and farm management of dairy mares and jennies. *JDS Communications*. 3(3). (2022). 234-237.

DEUGNIER M. [et al.] Myoepithelial cell differentiation in the developing mammary gland: progressive acquisition of smooth muscle phenotype. *Developmental Dynamics*. (1995). 107-117.

DOUCET S. [et al.] An overlooked aspect of the human breast: areolar glands in relation with breastfeeding pattern, neonatal weight gain, and the dynamics of lactation. *Early Human Development*. 88(2). (2012). 119–28.

DUSEK R. [et al.] Deficiency of the p53/p63 target perp alters mammary gland homeostasis and promotes cancer. *Breast Cancer Research*. 14(2). (2012). R65.

ECKERT F., VIRAGH P., SCHMID U. Coexpression of cytokeratin and vimentin intermediate filaments in benign and malignant sweat gland tumors. *Journal Cutaneous Pathology*. 21(2). (1994). 140–150.

EIGHMY J., SHARMA A., BLACKSHEAR P. *Chapter 21 - mammary gland*. In: ANDREW W. Suttie [et al.] eds. Boorman's Pathology Of The Rat. Second Edition. London, England: Elsevier, Academic Press, 2018. ISBN 978-0-12-391448-4. p. 369-388.

ESPINOSA DE LOS MONTEROS A. [et al.] Immunolocalization of the smooth muscle-specific protein calponin in complex and mixed tumors of the mammary gland of the dog: assessment of the morphogenetic role of the myoepithelium. *Veterinary Pathology*. 39(2). (2002). 247–256.

EVANS H. & CHRISTENSEN G. *The urogenital system.* In: EVANS H.& LAHUNTA A. Miller's Anatomy Of The Dog. Fourth Edition. Riverport: Missouri, Elsevier Saunders, 2013. ISBN 978-143770812-7. p 398.

EYSELBERGS M. [et al.] A rare cause of mastitis: idiopathic granulomatous mastitis. *Journal of The Belgian Society of Radiology.* 101(1). (2017). 2.

FANTUZ F. [et al.] Minor and potentially toxic trace elements in milk and blood serum of dairy donkeys. *Journal of Dairy Science*. 98(8). (2015). 5125–5132.

FIDLER I. & BRODEY R. A necropsy study of canine malignant mammary neoplasms. *Journal of The American Veterinary Medical Association*. 151(6). (1967). 710-715.

FOLEY J. [et al.] Parathyroid hormone-related protein maintains mammary epithelial fate and triggers nipple skin differentiation during embryonic breast development. *Development*. 128(4). (2001). 513–25.

FREEMAN C. [et al.] Idiopathic granulomatous mastitis: a diagnostic and therapeutic challenge. *American Journal of Surgery*. 214(4). (2017). 701-706.

GALISTEO J. & PEREZ-MARIN C. Factors affecting gestation length and estrus cycle characteristics in spanish donkey breeds reared in southern spain. *Theriogenology*. 74(3). (2010). 443-450.

GAMA A. [et al.] P63: a novel myoepithelial cell marker in canine mammary tissues. *Veterinary Pathology*. 40(4). (2003). 412-420.

GAMBA C. [et al.] Invasive micropapillary carcinoma of the mammary glands in a mare. *Veterinary Quarterly*. 31(4). (2011). 207–210.

GARCIA-RODIGUEZ J. & PATTULLO A. Idiopathic granulomatous mastitis: a mimicking disease in a pregnant woman: a case report. *BMC Research Notes*. 6(1). (2013). 95.

GARTNER F., GERALDES M., CASSALI G. DNA measurement and immunohistochemical characterization of epithelial and mesenchymal cells in canine mixed mammary tumors: putative evidence for a common histogenesis. *Veterinary Journal*. 158. (1999). 39-47.

GATTI V. [et al.] P63 at the crossroads between stemness and metastasis in breast cancer. *International Journal of Molecular Sciences*. 20(11). (2019). 2683.

GIACOMETTI L. & MONTAGNA W. The nipple and the areola of the human female breast. *The Anatomical Record.* 144(3). (1962). 191–197.

GIAMBRONE G. [et al.] Does TLS exist in canine mammary gland tumours? Preliminary results in simple carcinomas. *Veterinary Sciences*. 9(11). (2022). 628.

GOULABCHAND R. [et al.] Mastitis in autoimmune diseases: review of the literature, diagnostic pathway, and pathophysiological key players. *Journal of Clinical Medicine*. 9(4). (2020). 958.

GRANDI F. [et al.] Sebaceous metaplasia in a canine mammary gland non-infiltrative carcinoma with myoepithelial component. *Journal of Veterinary Diagnostic Investigation*. 23(6). (2011). 1230–1233.

GRIFFEY S. [et al.] Immunohistochemical reactivity of basal and luminal epithelium-specific cytokeratin antibodies within normal and neoplastic canine mammary glands. *Veterinary Pathology*. 30(2). (1993). 155-61.

GUGLIOTTA P. [et al.] Specific demonstration of myoepithelial cells by anti-alpha smooth muscle actin antibody. *Journal of Histochemistry & Cytochemistry*. 36(6). (1988). 659–663.

GULBAHAR M. [et al.] Mixed apocrine sweat gland tumor of the tail in a cow. *Veterinary Pathology*. 39(2). (2002). 281–285.

HAIHONG L. [et al.] Adult bone-marrow-derived mesenchymal stem cells contribute to wound healing of skin appendages. *Cell and Tissue Research*. 326(3). (2006). 725–736.

HASSAN E. [et al.] Ultrasonographic examination of mammary glands in lactating jennies (*Equua Asinus*). *Pakistan Veterinary Journal*. 36(1). (2016). 89–92.

HASSIOTOU F. & GEDDES D. Anatomy of the human mammary gland: current status of knowledge. *Clinical Anatomy*. 26(1). (2012). 29-48.

HAYES A. & MOONEY S. Feline mammary tumors. *Veterinary Clinics of North America: Small Animal Practice.* 15(3). (1985). 513-520.

HELLMÉN, E. & ISAKSSON, A. Immunohistochemical investigation into the distribution pattern of myoepithelial cells in the bovine mammary gland. *Journal of Dairy Research.* 64(2). (1997). 197–205.

HELMBOLDT C., JUNGHERR E., PLASTRIDGE W. The histophatology of bovine mastitis [online]. Storrs Agricultural Experiment Station Paper 45. EUA: University of Connecticut, College of Agriculture, Health and Natural Resources. (1953) (retrieved August 26th, 2023). In: https://digitalcommons.lib.uconn.edu/saes/45/

HENRY M. [et al.] Clinical and endocrine aspects of the oestrous cycle in donkeys (*equus asinus*). Journal of Reproduction and Fertility. *Supplement*. 35. (1987). 297-303.

HILLERTON J. & BERRY E. Treating mastitis in the cow – a tradition or an archaism. *Journal of Applied Microbiology*. 98(6). (2005). 1250–1255.

HIRAYAMA K. [et al.] Invasive ductal carcinoma of the mammary gland in a mare. *Veterinary Pathology*. 40(1). (2003). 86-91.

HOEPP N. *Chapter 44: mammary gland*. In: SHARKEY, L. [et al.] eds. Veterinary Cytology. First Edition. [S.I.] John Wiley & Sons, 2020. ISBN: 978-1-119-12570-9. p. 582-594.

HOVEY R. & TROTT J. Morphogenesis of mammary gland development. *Advances in experimental medicine and biology* .554(1). (2004). 219-228.

HUGHES C. & RUDLAND P. Appearance of myoepithelial cells in developing rat mammary glands identified with the lectins griffonia simplicifolia-1 and pokeweed mitogen. *The Journal Histochemistry Cytochemistry*. 38(11). (1990). 1647-1657.

HUGHES K., SCASE T., FOOTE A. Estrogen receptor and signal transducer and activator of transcription 3 expression in equine mammary tumors. *Veterinary Pathology*. 52(4). (2015). 631–634.

HUGHES, K. Development and pathology of the equine mammary gland. *Journal of Mammary Gland Biology and Neoplasia*. 26(2). (2020a). 121-134.

HUGHES, K. The known unknowns of equine mammary neoplasia. *Equine Veterinary Education*. 33(9). (2020b). 464-467.

HUMPHREYS R. [et al.] Apoptosis in the terminal endbud of the murine mammary gland: a mechanism of ductal morphogenesis. *Development*. 122(12). (1996). 4013-4022.

HURLEY W. [et al.] *Growth, Development and Involution*. In: FUQUAY J., FOX P. & MCSWEENEY P. Encyclopedia of Dairy Sciences. Second Edition. Amsterdam: Elsevier. (2011). ISBN: 978-0123744029. p. 338-345

HURT M. [et al.] Posttraumatic lobular squamous metaplasia of breast. An unusual pseudocarcinomatous metaplasia resembling squamous (necrotizing) sialometaplasia of the salivary gland. *Modern Pathology: An Official Journal of the United States and Canadian Academy of Pathology*. 1(5). (1988). 385-390.

JÚNIOR J. [et al.] Tubulopapillary carcinoma of the mammary gland in a mare. *Acta Scientiae Veterinariae*. 47(1). (2019). 432.

KAI-HONG J. [et al.] P63 expression pattern during rat epidermis morphogenesis and the role of p63 as a marker for epidermal stem cells. *Journal Of Cutaneous Pathology*. 34(2). (2007). 154–159.

KASKOUS S. & PFAFFL M. Milk properties and morphological characteristics of the donkey mammary gland for development of an adopted milking machine— a review. *Dairy*. 3(2). (2022). 233-247.

KAUSAR R., SARWAR S., HAYAT C. Gross and microscopic anatomy of mammary gland of dromedaries under different physiological conditions. *Pakistan Veterinary Journal*. (2001). 189 – 193.

KHAN S., MANJUSHA K., BANU A. Surgical affections of udder and teat in large animals. *Raksha Technical Review*. 9(2). (2020). 16 -21.

KOYAMA S. [et al.] The Nipple: a simple intersection of mammary gland and integument, but focal point of organ function. *Journal of Mammary Gland Biology and Neoplasia*.18(2). (2013). 121–131.

KUGLER W., GRUNENFELDER H., BROXHAM E. Donkey Breeds in Europe Inventory, Description, Need for Action, Conservation Report 2007/2008 [online]. Switzerland: Elli Broxham Monitoring Institute for Rare Breeds and Seeds in Europe. (2008). (retrieved August 26th 2023). In

http://www.agrobiodiversity.net/topic_network/donkey/Donkey/Report2007_2008.pdf

KULKA J. [et al.] Papillary lesions of the breast. *Virchows Arch*. 480(1). (2022). 65-84.

KURILJ A. [et al.] Complex mammary adenoma with sebaceous differentiation in a dog. *Journal of Comparative Pathology.* 146(2-3). (2009). 165–167.

LAUS F. [et al.] Mammary carcinoma in a mare: clinical, histopathological and steroid hormone receptor status. *Pferdeheilkunde*. 25(1). (2009). 18-21.

LEEUWEN I. [et al.] Cloning and cellular localization of the canine progesterone receptor: co-localization with growth hormone in the mammary gland. *The Journal of Steroid Biochemistry and Molecular Biology*. 75 (4–5). (2000). 219-228.

LI A. & KIRK L. Intraductal papilloma [online]. UK: StatPearls Publishing. (2022). (retrieved August 26th 2023). In: https://www.ncbi.nlm.nih.gov/books/NBK519539/

LI Q. [et al.] Donkey milk inhibits triple-negative breast tumor progression and is associated with increased cleaved-caspase-3 expression. *Food & Function*. 11(4). (2020). 3053-3065.

LI W. [et al.] Quantitative proteomic analysis of milk fat globule membrane (MFGM) proteins from donkey colostrum and mature milk. *Food & Function.* 10(7). (2019). 4254-4268.

LÍŠKA J. [et al.] Relationship between histology, development and tumorigenesis of mammary gland in female rat. *Experimental Animals.* 65(1). (2016). 1–9.

ŁOPUSZYŃSKI W. [et al.] Immunohistochemical expression of p63 protein and calponin in canine mammary tumours. *Research in Veterinary Science*. 123. (2019). 232–238.

LUDEWIG T. Histological investigations on the skin of the mammary gland of mares. *DTW - Deutsche tierarztliche Wochenschrift*. 104(11). (1997). 471-4.

MAESTRALE C. [et al.] A lympho-follicular microenvironment is required for pathological prion protein deposition in chronically inflamed tissues from scrapie-affected sheep. *Plos One*. (2013). 8(5).

MAHLER B. [et al.] Keratin 2e: a marker for murine nipple epidermis. *Cells Tissues Organs*. 176(4). (2004). 69–77.

MAIA L. A. [et al.] Cutaneous pythiosis in a donkey (*Equus Asinus*). In Brazil. *Journal of Veterinary Diagnostic Investigation*. 28(4). (2016). 436-439.

MARETTOVÁ, E. & MARETTA, M. Immunohistochemical study of the stromal cells in the lactating bovine mammary gland. *Folia Veterinaria*. 62(3). (2018). 29—35.

MARTINI M. [et al.] Quality of donkey mammary secretion during the first ten days of lactation. *International Dairy Journal*. 109. (2020). 10478

MASSO-WELCH, P. A. [et al.] A developmental atlas of rat mammary gland histology. *Journal of Mammary Gland Biology and Neoplasia*. 5(2). (2000). 165-185.

MCFADYEAN, J. The corpora amylacea of the mammary gland of the cow. *Journal of Comparative Pathology and Therapeutics*. 43. (1930). 291–300.

MCGEADY T. [et al.] *Male and female reproductive systems: development of the mammary gland.* In: MCGEADY T. [et al.]. Veterinary Embryology. First Edition. Nova Jersey, EUA: John Wiley & Sons. (2006). ISBN: 978-1405111478. p.263 – 267.

MIKKOLA M. P63 in skin appendage development*. Cell Cycle*. 6(3). (2007). 285-290.

MONTAGNA W. Histology and cytochemistry of human skin. XXXV: the nipple and areola. *British Journal of Dermatology*. 83. (1970). 2–13.

MORIOKA K., ARAI M., IHARA S. Steady and temporary expressions of smooth muscle actin in hair, vibrissa, arrector pili muscle, and other hair appendages of developing rats. *Acta Histochemica et Cytochemica*. 44(3). (2011). 141–153.

MORITONI S. [et al.] Availability of CD10 immunohistochemistry as a marker of breast myoepithelial cells on paraffin sections. *Modern Pathology*. 15(4). (2002). 397–405.

MOR-VAKNIN N. [et al.] Murine colitis is mediated by vimentin. *Scientific Reports*. 3. (2013). Article number: 1045.

MURAI A. [et al.] Mastitis caused by *Mycobacterium Kansasii* infection in a dog. *Veterinary Clinical Pathology*. 42(3). (2013). 377–381.

NICKERSON S. & AKERS R. *Mammary gland: anatomy*. FUQUAY, John W. ed. Encyclopedia of Dairy Sciences: Second Edition. Mississippi State, MS, USA: Elsevier, Academic Press, 2011. ISBN 978-0-12-374407-4. p. 328–337.

NICKERSON S. & SORDILLO L. Role of macrophages and multinucleate giant cells in the resorption of corpora amylacea in the involuting bovine mammary gland. *Cell and Tissue Research*. 240(2). (1985). 397–401.

NICKERSON S. [et al] Prevalence and ultrastructural characteristics of bovine mammary corpora amylacea during the lactation cycle. *Journal of Dairy Science*. 68(3). (1985). 709–717.

NIELSEN T. [et al.] Prepubertal exposure to cow's milk reduces susceptibility to carcinogen-induced mammary tumorigenesis in rats. *International Journal of Cancer.* 128(1). (2011). 12–20.

OBAIDAT N., ALSAAD K., GHAZARIAN D. Skin adnexal neoplasms-part 2: an approach to tumours of cutaneous sweat glands. *Journal of Clinical Pathology.* 60(2). (2006). 145–159.

OFTEDAL O. & DHOUAILLY D. Evo-devo of the mammary gland. *Journal of Mammary Gland Biology and Neoplasia.* 18(2). (2013). 105-20.

OKAMOTO Y. [et al.] Equine estrogen-induced mammary tumours in rats. *Toxicology Letters.* 193(3). (2010). 224–228.

PARSA R. [et al.] Association of p63 with proliferative potential in normal and neoplastic human keratinocytes. *Journal of Investigative Dermatology.* 113(6). (1999). 1099–1105.

PATTISON I. Studies on experimental streptococcal mastitis: vi. Histological examination of teats of affected goats. *Journal of Comparative Pathology and Therapeutics*. 62. (1952). 1-5.

PEUHU E. [et al] Epithelial vimentin plays a functional role in mammary gland development. *Development*. 144(22). (2017). 4103–4113.

PILLA R. [et al.] Hygienic and health characteristics of donkey milk during a follow-up study. *Journal of Dairy Research*. 77(4). (2010). 392–397.

PODICO G. [et al.] A novel *Streptococcus* species causing clinical mastitis in a pregnant donkey. *Journal of Veterinary Diagnostic Investigation*. 33(5). (2021). 979-983.

QUARESMA M. & NÓVOA M. *The reproductive system.* In EVANS, L. & CRANE, M. The Clinical Companion of the Donkey. 1st edition. UK: The Donkey Sanctuary. (2018). ISBN: 9781789013900. pp 73-86.

QUARESMA M. [et al.] Pedigree and herd characterization of a donkey breed vulnerable to extinction. *Animal: An International Journal of Animal Bioscience.* 8(3). (2014). 354–359.

QUARESMA M. [et al.] The donkey breed asinina de miranda [online]. Portugal: Revista Portuguesa De Ciências Veterinárias. (2005). 173-177. (retrieved August 26th 2023). In: https://www.academia.edu/50348773/A_ra%C3%A7a_Asinina_de_Miranda_The_donkey_breed_Asinina_de_Miranda

RAMALHO L. [et al.] The expression of p63 and cytokeratin 5 in mixed tumors of the canine mammary gland provides new insights into the histogenesis of these neoplasms. *Veterinary Pathology*. 43(4). (2006). 424–429.

RAMOS-VARA J. Technical aspects of immunohistochemistry. *Veterinary Pathology.* 42(4). (2005). 405-426.

RAPOSIO E. [et al.] Characterization of multipotent cells from human adult hair follicles. *Toxicology in Vitro: An International Journal Published in Association with BIBRA*. 21(2). (2007). 0–323.

RASOTTO R. [et al.] The dog as a natural animals model for study of the mammary myoepithelial basal cell lineage and its role in mammary carcinogenesis. *Journal of Comparative Pathology*. 151(2-3). (2014). 166–180.

RATH-WOLFSON L. [et al.] The phenomen of squamous metaplasia in benign and malignant lesions of the breast. *Conexiuni Medicale*. 5(3). (2010). 29-44.

REDDICK R., JENNETTE J., ASKIN F. Squamous metaplasia of the breast: an ultrastructural and immunologic evaluation. *American Journal of Clinical Pathology.* 84(4). (1985). 530–533.

REESINK H. [et al.] Malignant fibrous histiocytoma of the mammary gland in a mare. *Equine Veterinary Education*. 21(9). (2009). 467–472.

REIS-FILHO J. [et al.] P63 expression in normal skin and usual cutaneous carcinomas. *Journal of Cutaneous Pathology*. 29(9). (2002). 517–523.

RIBA M. [et al.] From *corpora amylacea* to wasteosomes: history and perspectives. *Ageing Research Reviews*. 72. (2021). Article number: 101484.

RIOS A. [et al.] In situ identification of bipotent stem cells in the mammary gland. *Nature*. 506. (2014). 7488.

ROWSON A. [et al.] Growth and development of the mammary glands of livestock: a veritable barnyard of opportunities. *Seminars in Cell Developmental Biology*. 23(5). (2012). 557–66.

RUSSO I. & RUSSO J. Developmental stage of the rat mammary gland as determinant of its susceptibility to 7,12-dimethylbenz[a]anthracene. *Journal of National Cancer Institute.* 61(6). (1978). 1439-49.

RUSSO J. & RUSSO I. Atlas and histologic classification of tumors of the rat mammary gland. *Journal of Mammary Gland Biology and Neoplasia*. 5(2). (2000). 187-200.

SABIZA S. [et al.] Surgical treatment of a mammary gland comedocarcinoma in an arabian mare: post-operative management, and histopathological and immunohistochemical features. *Equine Veterinary Education.* 33(9). (2020). 321-325.

SALIMEI E. & FANTUZ F. Equid milk for human consumption. *International Dairy Journal.* 24(2). (2012). 130–142.

SÁNCHEZ-CÉSPEDES R. [et al.] Use of CD10 as a marker of canine mammary myoepithelial cells. *The Veterinary Journal (London, England 1997*). 195(2). (2013). 192-199.

SARAIVA A., GÄRTNER F., PIRES M. Expression of P63 normal canine skin and primary cutaneous glandular carcinomas. *Veterinary Journal (London, England 1997).* 177(1). (2008). 136–140.

SARNO E. [et al.] Microbiological quality of raw donkey milk from Campania Region. *Italian Journal of Animal Science.* 11(3). (2012). 266- 269.

SATO A. [et al.] Single follicular unit transplantation reconstructs arrector pili muscle and nerve connections and restores functional hair follicle piloerection. *The Journal of Dermatology*. 39(8). (2012). 1-6.

SHANK A. Clinical commentary - mare mammary neoplasia: difficulties in diagnosis and treatment. *Equine Veterinary Education.* 21(9). (2009). 475–477.

SHIMOMURA Y. [et al.] P-cadherin is a p63 target gene with a crucial role in the developing human limb bud and hair follicle. *Development*. 135(4). (2008). 743–753.

SORDILLO L. & NICKERSON S. Growth patterns and histochemical characterization of bovine mammary corpora amylacea. *Journal of Histochemistry & Cytochemistry.* 34(5). (1986). 593–597.

SORENMO K. [et al.] Development, anatomy, histology, lymphatic drainage, clinical features, and cell differentiation markers of canine mammary gland neoplasms. *Veterinary Pathology*. 48(1). (2010). 85–97.

SOUROULLAS K., ASPRI M., PAPADEMAS P. Donkey milk as a supplement in infant formula: benefits and technological challenges. *Food Research International*. 109. (2018). 416–425.

SOUTO E. [et al.] Mastitis by *Pythium Insidiosum* in mares. *Acta Scientiae Veterinariae*. 47(1). (2019). 387.

SPAAS J. [et al.] Stem/progenitor cells in non-lactating versus lactating equine mammary gland. *Stem Cells and Development*. 21(16). (2012). 3055–3067.

SPADARI A. [et al.] Case report - mammary adenoma in a mare: clinical, histopathological and immunohistochemical findings. *Equine Veterinary Education*. 20(1). (2008). 4–7.

SPREGA (Sociedade Portuguesa de Recursos Genéticos Animais): Asininos - raça burro de miranda [online]. Vale de Santarém, Portugal: Ruralbit. [retrieved September 9, 2022]. In: https://www.sprega.com.pt/conteudo.php?idesp=asininos&idraca=Burro%20de%20Miranda

TANG, D. Intermediate filaments in smooth muscle. *American journal of physiology. Cell physiology*. 294(4). (2008). 869-878.

TARTOR Y. [et al.] Equine pythiosis in egypt: clinicopathological findings, detection, identification and genotyping of pythium insidiosum. *Veterinary Dermatology.* 31(4). (2020). 298-e73.

TONITI P. [et al.] AE1/AE3, vimentin and p63 immunolocalization in canine mammary gland tumours: roles in differentiation between luminal epithelial and myoepithelial lineages. *Asian Pacific Journal of Cancer Prevention: APJCP*. 11(1). (2010). 227-230.

TSUJITA-KYUTOKU M. [et al.] P63 expression in normal human epidermis and epidermal appendages and their tumors. *Journal of Cutaneous Pathology.* 30(1). (2003). 11–17.

TURINI L. [et al.] Evaluation of jennies' colostrum: igg concentrations and absorption in the donkey foals: A preliminary study. *Heliyon*. 6(8). (2020). e04598.

VALLE E. [et al.] Effect of farming system on donkey milk composition. *Journal of the Science of Food and Agriculture.* 98(7). (2018). 2801-2808.

VOS J. [et al.] Immunohistochemistry with keratin, vimentin, desmin and a-smooth muscle actin monoclonal antibodies in canine mammary gland: benign mammary tumours and duct ectasias. *The Veterinary Quarterly.* 15(3). (1993a). 89-95.

VOS J. [et al.] Immunohistochemistry with keratin, vimentin, desmin, and alpha-smooth muscle actin monoclonal antibodies in canine mammary gland: normal mammary tissues. *The Veterinary Quarterly.* 15(3). (1993c). 102- 107.

VOS, J. [et al.] Immunohistochemistry with keratin, vimentin, desmin, and alpha-smooth muscle actin monoclonal antibodies in the canine mammary gland: malignant mammary tumours. *The Veterinary Quarterly.* 15(3). (1993b). 96–102.

WANG R., Li Q., Tang D. Role of vimentin in smooth muscle force development. *American Journal of Physiology: Cell physiology*. 291(3). (2006). 483-489.

WATSON C.& WALID K. Mammary development in the embryo and adult: new insights into the journey of morphogenesis and commitment. *Development* 147(22). (2020). 1-14.

WEBER, E. [et al.] Self-organizing hair peg-like structures from dissociated skin progenitor cells: new insights for human hair follicle organoid engineering and turing patterning in an asymmetric morphogenetic field. *Experimental Dermatology.* 28(4). (2019). 355-366.

YALLOWITZ A. [et al.] P63 is a prosurvival factor in the adult mammary gland during post-lactational involution, affecting pi-mecs and erbb2 tumorigenesis. *Cell Death & Differentiation*. 21(4). (2014). 645–654.

ZAPPULLI V. [et al.] Surgical Pathology of Tumors of Domestic Animals: *Vol 2-Mammary Tumors.* 1st edition. Germany: Davis- Thompson Foundation. (2019). pp 1-26 and 62-72. ISBN: 978-1733749114

ZHANG X. [et al.] Label-free based comparative proteomic analysis of whey proteins between different milk yields of Dezhou donkey. *Biochemical and Biophysical Research Communications.* 508(1). (2018). 237-242.

ZHAO Y. [ et al.] Antimicrobial susceptibility of bacterial isolates from donkey uterine infections, 2018–2021. *Veterinary Sciences*. 9(2). (2022). 67.

ZUCCARI D., SANTANA A., ROCHA N. Expression of intermediate filaments in canine mammary tumor diagnosis. *Brazilian Archive Veterinary Medicine Animal Science*. 54(6). (2002). 586-91.

## VIII – Appendix

Appendix 1

# Histological and immunohistochemical characterization of the donkey (*Equus asinus*) mammary gland

Jesus R[1], Chafirovitch-Radar A[2], Pires MA[2,3], Payan-Carreira R,[4] Nóvoa M[5], Quaresma M[2], Gama A[2,3]*

[1]Veterinary Medicine, Escola de Ciências e Tecnologia, Universidade de Évora, Évora, Portugal; [2]Animal and Veterinary Research Centre (CECAV), UTAD, and Associate Laboratory for Animal and Veterinary Science (AL4Animals), Vila Real, Portugal; [3]Department of Veterinary Sciences, School of Agrarian and Veterinary Sciences (ECAV), UTAD, Vila Real, Portugal; [4]Comprehensive Health Research Centre, Departmento Medicina Veterinária, Escola de Ciências e Tecnologia, Universidade de Évora, Évora, Portugal; [5]Associação para o Estudo e Proteção do Gado Asinino (AEPGA), Miranda do Douro, Portugal; agama@utad.pt

## INTRODUCTION

A comprehensive characterization of the donkey mammary gland (MG) histology can support the investigation of pathological processes affecting this organ, such as mastitis or proliferative lesions. Given that scarce information is available on this topic, the present study aimed to evaluate the histomorphological characteristics of the asinine MG.

## MATERIALS AND METHODS

Sixty-five MGs collected from jennies (0 to 37 years; mean 17.9) during post-mortem examination were formalin-fixed and processed for histopathology. In addition, immunohistochemistry was performed on sixteen samples using anti-cytokeratin AE1AE3, α-smooth muscle actin, p63, calponin and vimentin antibodies.

## RESULTS

A total of 65 donkey MG were analysed, presenting a structural organization comparable to mares, with two paired mammary complexes exhibiting distinct histological morphologies (prepubertal, inactive, fully developed lactating and involuting MG). The immunohistochemical markers showed similar expression patterns to other species, confirming these cell markers as suitable phenotypical biomarkers in donkeys.

Although with no macroscopic lesions, 10/65 MG (15.4%) presented the following histological alterations: papillomatosis, characterized by intraductal epithelial papillary projections, associated with ductal ectasia (n=2; 3.1%); cystic apocrine metaplasia, characterized by cystically dilated ducts lined by benign apocrine epithelium (n=1; 1.5%) and sebaceous and apocrine metaplasia (n=6; 9.2% and n=3; 4.6%, respectively), with multiple alterations found in two animals.

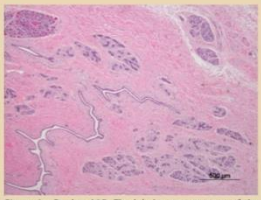

Figure 1 - Donkey MG. The lobular arrangement of the mammary acini and ducts. H&E staining.

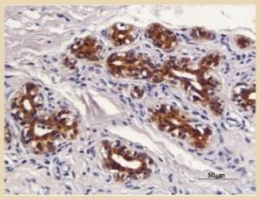

Figure 2 - Donkey non-lactating MG. CK AE1AE3 immunostaining: luminal cells cytoplasm highly stained. Gill's haematoxylin counterstain.

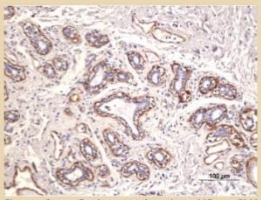

Figure 3 - Donkey non-lactating MG. α-SMA immunostaining of the myoepithelial cell layer. Gill's haematoxylin counterstain.

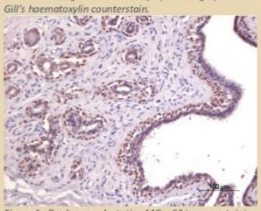

Figure 4 - Donkey non-lactating MG. p63 immunostaining of myoepithelial cells nuclei. Gill's haematoxylin counterstain.

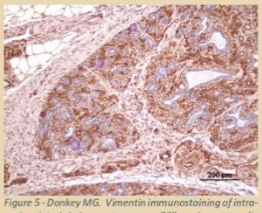

Figure 5 - Donkey MG. Vimentin immunostaining of intra- and interlobular stroma. Gill's haematoxylin counterstain.

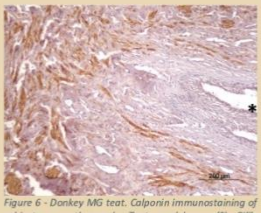

Figure 6 - Donkey MG teat. Calponin immunostaining of sphincter smooth muscle. Teat canal lumen (*). Gill's haematoxylin counterstain.

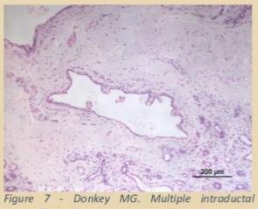

Figure 7 - Donkey MG. Multiple intraductal epithelial papillary projections, associated with duct ectasia. H&E staining.

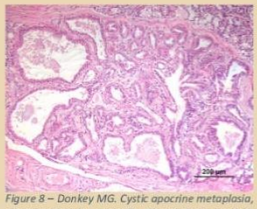

Figure 8 – Donkey MG. Cystic apocrine metaplasia, characterized by cystically dilated ducts lined by benign apocrine epithelium. H&E staining.

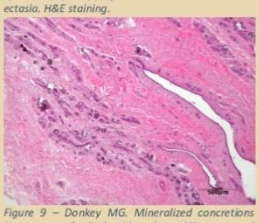

Figure 9 – Donkey MG. Mineralized concretions (psammoma bodies) with a basophilic core and concentric striations. H&E staining.

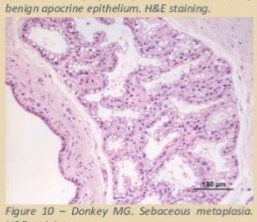

Figure 10 – Donkey MG. Sebaceous metaplasia. H&E staining.

Mineralized concretions (psammoma bodies) were frequently observed (n=30;46.1%). In addition, mononuclear inflammatory (n=12; 28,6%) and eosinophils (n=3; 7,4%) infiltrates were observed in mammary parenchyma.

## CONCLUSIONS

This study presents a histological characterization of a series of donkey MGs, confirming the morphological and immunohistochemical similarities with other mammals, especially mares. We believe that comparative studies on the biopathology of MG focusing on donkeys may provide new insights on mammary tumourigenesis, with potential application to other species.

This work was financed by national funds through FCT – Portuguese Foundation for Science and Technology, within the scope of the projects UIDB/CVT/00772/2020 (CECAV) and LA/P/0059/2020 (AL4AnimalS) and PhD grant UI/BD/150839/2021 (ARC).

*Appendix 1 – Scientific poster: Congress of the ECVP/ESVP/ECVCP/ESVCP – Lisbon 2023.*